

1 **Reply to the comments by Referees**

2 -----
3
4 **To Associate Editor and Referees,**

5
6 We appreciate you reading our paper carefully and giving valuable comments and suggestions again. We
7 have considered your recommendations for revisions and made the necessary changes. The major points
8 that we deal with in the revised manuscript are as follows:
9

- 10 1. Following the advice of the Referee #2, we have added Table 1 to show representative pressure
11 levels of each of the retrieval grid layers of GOSAT/TANSO-FTS thermal infrared (TIR) version
12 1 (V1) Level 2 (L2) CO₂ product. (We have already addressed this in AMTD.)
- 13 2. Relating to the above, we have referred to the retrieval grid layers by the representative pressure
14 levels throughout the text. (We have already addressed this in AMTD.)
- 15 3. Following the advice of the Referee #1, we have added Table 2 to present bias values of
16 GOSAT/TANSO-FTS TIR V1 L2 CO₂ data against CONTRAIL CME CO₂ data to which TIR
17 CO₂ averaging kernel functions were applied. It could help readers see Figure 6.
- 18 4. Following the advice of the Referee #1, we have added Table 3 to present mode values of
19 frequency distributions of differences in monthly averaged CO₂ concentrations between original
20 or bias-corrected TIR and NICAM-TM CO₂ data and numbers of data categorized into the mode
21 values and all 2.5° gridded data used for comparisons. It could help readers see Figure 7.

22
23 Individual responses to the Referees' comments are listed below.
24

25 **Reply to Referee #1,**

26
27 *The paper assesses biases in satellite-retrieved CO₂ concentrations at the lower and middle*
28 *troposphere from GOSAT/TANSO-FTS TIR V1 product by comparing them with precise aircraft*
29 *measurements by CONTRAIL CME, followed by global comparisons of bias-corrected CO₂*
30 *concentrations with model-simulated CO₂ by NICAM-TM. The authors found that the TIR data had*
31 *negative biases of 1-1.5% against the aircraft measurements and bias-corrected TIR data showed*
32 *generally good agreement with the NICAM-TM CO₂ data, which demonstrated the validity of the*
33 *bias-correction values.*

34 *Observational CO₂ data in the free troposphere is still limited, and CO₂ profiles from high-resolution*
35 *GOSAT TIR spectra will help to elucidate CO₂ variations in the free troposphere with its global*
36 *coverage. Bias estimation of satellite-based CO₂ products is highly important for data users and*
37 *further analysis of CO₂ fluxes by atmospheric inversion/data-assimilation studies. The paper is*

1 generally well written, and I recommend accepting it for publication after the comments listed below
2 have been addressed.

3
4 *General comments:*

5 *1. Results section: The paper presents comparisons between the original TIR data and CONTRAIL*
6 *CME data and between bias-corrected TIR data and NICAM-TM data. But the expressions of the*
7 *evaluations are often qualitative, such as “relatively low”, “tend to be larger”, “slightly increase”,*
8 *“nearly identical”, “close to zero” without any supporting numbers. Although one can see tendencies*
9 *on the plots, I would recommend illustrating the point with some numbers and add a table with*
10 *quantitative values to explain the results clearly. The authors do not need to write all related numbers,*
11 *but at least it would be better to write statistic values related to Figure 7, one of the main plots, to*
12 *show the validity of the bias-correction values quantitatively. Statistic values in a table or the main*
13 *text may help readers to follow the discussion. They can be mode values (or medians), standard*
14 *deviations, kurtoses and skewnesses of frequency distributions, the total number of data pairs, or*
15 *whatever the authors need to describe Figure 7.*

16
17 *Reply:*

18 We totally agree with you. As described above, we have added Table 2 and Table 3 to present
19 specific values of what we focused on in Figure 6 and Figure 7, respectively. In the revised
20 manuscript, we have referred to Table 2 and Table 3 to clarify points of discussions related to
21 Figure 6 and Figure 7. We have also referred to specific values presented in Table 2 and Table 3
22 in the main text of the revised manuscript. We appreciate your comment.

23
24 *2. “East Asia” in abstract and discussion section: The authors conclude that one of the reasons of the*
25 *overcorrection in JJA/low latitudes (0S-20N)/upper MT region is that the correction values were*
26 *determined by using the data over East Asian airports. Since the authors write this finding to the*
27 *abstract, this conclusion is thought to be important for the paper. But the explanation (p.10, L34 - L11,*
28 *L8) is not clear enough to understand why data in the East Asia region strongly affects to the 0-20N*
29 *bias correction. Usually, Asia in 20S-20N is called Southeast Asia (or part of South India). Do the*
30 *authors mean “Southeast Asia” rather than “East Asia”? Or if the East Asian data truly affects the 0-20N*
31 *bias-correction values via atmospheric transport, please give more explanation and references.*

32
33 *Reply:*

34 We greatly appreciate you pointing out this. We wrote “East Asia” incorrectly in the sentences
35 where we should have written “Southeast Asia” in the manuscript. We intended to say that the
36 bias-correction values in low latitudes (20°S–20°N) in the JJA season in 2010 were determined
37 on the basis of comparisons over the three airports over Southeast Asia: BKK (Bangkok), SIN
38 (Singapore), and CGK (Jakarta). In the revised manuscript, we have replaced “East Asia” with

1 “Southeast Asia” throughout the text and described these specific airports in the discussion part.

2
3 *Specific comments:*

4 *Page 3, Section 2, TIR data: Does the TIR product include nighttime data as well as daytime data? I*
5 *suggest writing time of the observations briefly somewhere in this section.*

6
7 Reply:

8 The TIR products of GOSAT/TANSO-FTS include data obtained both in daytime and nighttime.

9 Following your suggestion, we have stated this clearly in the revised manuscript as follows:

10 “The TIR band of TANSO-FTS makes observations both in daytime and nighttime, unlike the
11 SWIR band.”

12
13 *Page 4, Section 3, NICAM-TM data: NICAM-TM inversion with CONTRAIL data was conducted for*
14 *the period 2006-2008 (Niwa et al., 2012). It should be explained briefly how the 2010-2012 CO₂ data*
15 *was calculated by NICAM-TM.*

16
17 Reply:

18 We agree with you. As you pointed out, the NICAM-TM inversion simulation that was conducted
19 in Niwa et al. (2012) used CONTRAIL and surface CO₂ data in 2006–2008 to estimate the
20 natural flux of CO₂. The NICAM-TM CO₂ data used here were generated by using the estimated
21 CO₂ natural flux (fixed for 2010–2012) and year-dependent CO₂ fluxes from fossil fuel and
22 biomass burning emissions (considering their yearly trends). Following your suggestion, we have
23 added more explanation of the NICAM-TM CO₂ inversion as follows:

24 “In this study, simulation of NICAM-TM used inter-annually varying flux data of fossil fuel
25 emissions (Andres et al., 2013) and biomass burnings (van der Werf et al., 2010), and the residual
26 natural fluxes from the inversion of Niwa et al. (2012), which mostly represent fluxes from the
27 terrestrial biosphere and oceans. The inversion analysis of Niwa et al. (2012) was performed for
28 2006–2008 and the three-year-mean fluxes were used in this study.”

29 We appreciate your comment.

30
31 *Page 5, line 24, “the number of pairs”:* *Could the authors show the number of pairs which finally*
32 *used for the comparisons for each latitude bands?*

33
34 Reply:

35 Following your suggestion, we have described the numbers of coincident pairs of TIR and
36 CME_AK CO₂ profiles for each of the four latitude bands in the fourth paragraph of Chapter 4.1
37 in the revised manuscript:

38 “The numbers of coincident pairs of TIR and CME_AK CO₂ profiles varied depending on

1 latitude band and season. The largest number of coincident pairs was obtained in the latitude band
 2 of 20°N–40°N including Narita airport, where 506–2501 pairs were obtained. 63–310 and
 3 77–472 coincident pairs were obtained at 40°S–20°S and 40°N–60°N, respectively. The
 4 comparison area for low latitudes was extended to a band of 20°S–20°N, because the number of
 5 coincident pairs in that region was smaller (0–341) than in other latitude bands; nevertheless,
 6 there were no coincident pairs at 20°S–20°N in the JJA seasons of 2011 and 2012. The number of
 7 coincident pairs was smallest (0–30) at 20°S–0° and no data were collected there after September
 8 2010. Thus, all bias-correction values for 20°S–20°N after the SON season of 2010 were
 9 determined based on data from 0°–20°N.”

10 The below-attached table shows the numbers of the coincident pairs for each season for each
 11 latitude band.

		40°S–20°S		20°S–0°/0°–20°N		20°N–40°N		40°N–60°N	
2010, MAM	2010, JJA	63	75	27/114	30/95	1305	2501	472	161
2010, SON	2010, DJF	128	114	0/172	6/155	2133	1588	454	132
2011, MAM	2011, JJA	209	183	0/49	0/0	506	1255	77	227
2011, SON	2011, DJF	179	78	0/137	0/234	1529	1049	199	253
2012, MAM	2012, JJA	310	105	0/49	0/0	748	1815	418	406
2012, SON	2012, DJF	145	166	0/31	0/341	2045	1664	326	119

13
 14 *Page 7, line 10, “On a global scale, the seasonality of negative biases was not clear, given the*
 15 *relatively large 1-σ standard deviations, although these biases tended to be larger in the spring*
 16 *hemisphere than in the fall hemisphere.”: The sentence is not clear. Does this mean the negative biases*
 17 *had measurable spring-fall seasonality, but it was not statistically significant due to the large*
 18 *standard deviations? Or actually, the biases had no seasonality?*

19
 20 Reply:

21 In northern middle latitudes (20°N–40°N), negative biases in TIR CO₂ data were larger in spring
 22 (MAM) and summer (JJA) than in fall (SON) and winter (DJF). On a global scale from
 23 40°S–60°N, any statistically significant seasonality was not found in negative biases in TIR CO₂
 24 data against CONTRAIL CME_AK CO₂ data. In Table 2 of the revised manuscript, we have
 25 presented bias values of TIR CO₂ data against CME_AK CO₂ data in each season at 541–464
 26 hPa and 464–398 hPa (corresponding to layers 5–6) to make readers refer to specific values that
 27 we focused on.

28
 29 *Page 7, line 26, “negative biases of TIR CO₂ data against NICAM-TM CO₂ data in all seasons slightly*
 30 *increased over time”: Is there no possibility that small trend error in NICAM-TM CO₂ could attribute*
 31 *the bias increase in Fig.7? The NICAM-TM natural fluxes were estimated for the period 2006-2008,*
 32 *which is different from the target period of this article. In other words, does the NICAM CO₂ have no bias*
 33 *in trends against CONTRAIL CME data? The authors can confirm it by plotting NICAM-TM CO₂ data*
 34 *against CONTRAIL CME data like Fig.6.*

1
2
3
4
5
6
7
8
9
10
11
12
13
14
15
16
17
18
19
20
21
22
23
24
25
26
27
28
29
30
31
32
33

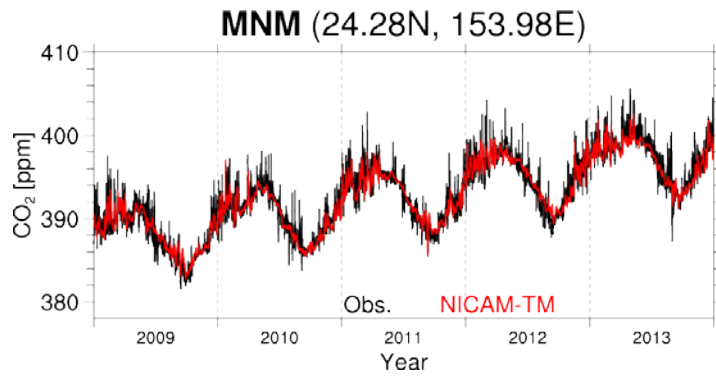
Reply:

As explained above, the NICAM-TM inversion simulation that was conducted in Niwa et al. (2012) used CONTRAIL and surface CO₂ data in 2006–2008 to estimate the natural flux of CO₂. When calculating CO₂ concentrations in 2010–2012, the mean inversion fluxes were cyclically used, but fossil fuel and biomass burning CO₂ fluxes used were varied inter-annually. We confirmed that the growth rate of the calculated NICAM-TM CO₂ concentrations for 2010–2012 is reasonable (2.4 ppm/yr) judging from an observation-based growth rate (2.2 ppm/yr), which is partly contributed by the fact that there were no major El Nino events for both the periods. The below-attached figure shows comparison between the NICAM-TM CO₂ simulations and observations at the surface station at Minamitorishima, which demonstrates the validity of the NICAM-TM CO₂ simulations. As Figure 6 is based on one-by-one coincident GOSAT–CME_AK CO₂ comparisons over airports selected by applying the thresholds of a 300-km distance and a 72-h time difference, we think that it is inappropriate to plot comparisons between 2.5°-gridded NICAM-TM and CME CO₂ data on the same figure. Alternatively, we have described the specific comparison in CO₂ growth rates between NICAM-TM simulation and surface observation data as follows:

“Furthermore, the CO₂ forward simulation of NICAM-TM for 2010–2012 showed a good agreement with in-situ CO₂ observations not only in seasonal cycles but also in trends in spite of using the fluxes optimized for 2006–2008; the simulated growth rate at the Minamitorishima station (e.g., Wada et al., 2011), which is one of the global stations of the Global Atmospheric Watch (GAW), was 2.4 ppm/yr for 2010–2012, while the growth rate based on in-situ observations was 2.2 ppm/yr.”

“In addition, negative biases of TIR CO₂ data against NICAM-TM CO₂ data in all seasons slightly increased over time, judging from the mode values presented in the top left boxes of Table 3, although the increase in negative biases was not much evident as in the comparisons over airports shown in Figure 6; this may be partly because of slightly high growth rate of NICAM-TM simulations (2.4 ppm/yr) compared to in-situ observations (2.2 ppm/yr).”

We greatly appreciate your comment.



1
2
3 Reference figure. Time-series of observed (black) and simulated (red) CO₂ concentrations at the
4 surface station at Minamitorishima. The observation data presented here were taken from the
5 World Data Center for Greenhouse Gases (WDCGG). The observations have been conducted by
6 JMA under the program of WMO/GAW. We would like to acknowledge the staff that supports the
7 observations.

8
9 *Page 9, line 5, other sources of negative biases: I'm not familiar with retrieval algorithms, but would*
10 *any errors in cloud detection process cause retrieval errors in the low latitudes with enhanced*
11 *convective activity? And H₂O or O₃ do not affect the CO₂ retrieval results?*

12
13 Reply:

14 We appreciate your comment. As you pointed out, uncertainties in H₂O and O₃ data could also
15 affect CO₂ retrievals, as shown in Figure 7(b) and (c) of Saitoh et al. (2009). The TIR V1 CO₂
16 retrieval algorithm (Saitoh et al., 2016) simultaneously retrieves H₂O and O₃ with CO₂, which
17 could decrease the effect of their uncertainties on CO₂ retrieval results. However, water vapor is
18 abundant in the tropics, so that we cannot completely deny the possibility of the effect of H₂O
19 uncertainty on CO₂ retrieval results. Similarly, error in the judgement of cloud contamination
20 may affect CO₂ retrieval results. We have added this point to the discussion part of the revised
21 manuscript as follows:

22 “Although the effect of uncertainty in H₂O data on CO₂ retrieval results could be also decreased
23 by simultaneous retrieval of H₂O with CO₂ in the TIR V1 algorithm, water vapor is abundant in
24 the tropics, so that we cannot deny the possibility of its effect on CO₂ retrieval results. Similarly,
25 error in the judgement of cloud contamination in low latitudes with high cloud occurrence
26 frequency may affect CO₂ retrieval results.”

27
28 *Page 10, lines 29-30, “The CME data that determined the bias-correction values of the 20°S–20°N*
29 *latitude band were concentrated in East Asia”:* I was confused with this sentence. Please see my
30 *general comment #2.*

1 Reply:

2 As described above, we have replaced “East Asia” with “Southeast Asia” throughout the text. In
3 the revised manuscript, we have listed specific airports (BKK, SIN, and CGK) where most CME
4 data were obtained in the latitude band of 20°S–20°N as follows:

5 “The CME data that determined the bias-correction values of the 20°S–20°N latitude band were
6 concentrated in Southeast Asia, as illustrated in Figure 1: BKK (Bangkok), SIN (Singapore), and
7 CGK (Jakarta).”

8 We appreciate your comment.

9
10 *Page 10, line 34 – page 11, line 1, “in most areas at 0°–20°N, and the negative biases were largest*
11 *near airport locations in East Asia.”: Same as above. Please see my general comment #2.*

12
13 Reply:

14 As described above, we have replaced “East Asia” with “Southeast Asia” throughout the text. We
15 appreciate your comment.

16
17 *Page 11, lines 12-13, “More in-situ CO₂ data in the upper atmosphere in low latitudes”: Hiaper*
18 *Pole-to-Pole Observations (HIPPO) project observed latitudinal distributions of CO₂ concentrations*
19 *in the free troposphere over the Pacific Ocean where mostly clean during 2009 to 2011 (e.g. Wofsy et al.,*
20 *2011). The dataset has been used for transport model or satellite data validation (e.g. Wecht et al.,*
21 *2012; Kulawik et al., 2013). The comparison with HIPPO data is out of the scope of this paper, but if*
22 *the authors found some problems in using HIPPO data for validation, please write it in the discussion*
23 *section or the introduction section.*

24 *Wofsy, S. C. et al.: HIAPER Pole-to-Pole Observations (HIPPO): fine-grained, global-scale*
25 *measurements of climatically important atmospheric gases and aerosols, Phil. Trans. Roy. Soc. A:*
26 *Math. Phys. Eng. Sci., 369, 2073–2086, doi:10.1098/rsta.2010.0313, 2011.*

27
28 Reply:

29 We agree with you. The reason why we did not use HIPPO data in this study is that HIPPO
30 campaign observations were conducted for limited periods (October–November in 2009,
31 March–April in 2010, June–July in 2011, and August–September in 2011, after starting the
32 regular operation of GOSAT) in limited areas (mainly over the Pacific Ocean), so that they are
33 not suitable for evaluating season- and latitude-dependent biases in GOSAT/TANSO-FTS TIR
34 CO₂ data. As you pointed out, however, HIPPO data themselves are useful to validate CO₂
35 vertical profiles observed by satellite-borne sensors and simulated in models. Following your
36 advice, we have touched on HIPPO data in the discussion part of the revised manuscript as
37 follows:

38 “Although HIAPER Pole-to-Pole Observations (HIPPO) data (Wofsy et al., 2011) are not

1 suitable for a comprehensive validation study as in this study due to their limited observation
2 periods, HIPPO CO₂ data are useful to validate CO₂ vertical profiles observed by
3 satellite-borne sensors and simulated in models (Kulawik et al., 2013).”

4 We appreciate your comment.
5

6 *Page 11, line 17, “Reconsideration of the setting of retrieval grid layers ...”: Why do the authors think*
7 *the current setting of retrieval grid layers might not be suitable for retrievals and reconsideration might*
8 *solve it?*
9

10 Reply:

11 Total degree of freedom (defined as the trace of averaging kernel matrix) does not depend on the
12 setting of retrieval grid layers theoretically. In this situation, partial degree of freedom for each
13 retrieval grid layer (defined here as the diagonal element of averaging kernel matrix
14 corresponding to each retrieval grid layer, see Saitoh et al. (2016)) should decrease as the number
15 of retrieval grid layers increases. As illustrated in reference figure attached in Authors’ reply to
16 Referee #2, the total degrees of freedom of GOSAT/TANSO-FTS TIR V1 CO₂ data are on
17 average 1.1–2.2 (depending on latitude and season), which means that we can derive information
18 on CO₂ concentrations in more than 1–2 vertical layers independently from observations by the
19 TIR band. In the TIR V1 Level 2 CO₂ retrieval algorithm, we have set 28 vertical grid layers.
20 Judging from the total degree of freedom of the TIR CO₂ data and the relatively small partial
21 degree of freedom for each vertical grid layer, we think we should reconsider the setting of
22 retrieval grid layers.
23

24 *Page 11, line 20, “during the JJA seasons of 2011 and 2011”: Does this mean “2011 and 2012”?*
25

26 Reply:

27 We have modified the sentence. We appreciate you pointing out our mistake.
28

29 *Figs.3: The Y axis is described in altitude, not in pressure as seen in the following plots. For easy*
30 *reference, I would suggest adding a 2nd Y axis in pressure or adding a column in Table 1 to show*
31 *altitude [km] for each pressure levels. (Rough altitudes from International Standard Atmosphere or*
32 *the same kind might be enough for this purpose.*
33

34 Reply:

35 Following your suggestion, we have added a second vertical axis (y-axis) in pressure in Figure 3
36 of the revised manuscript. Here, we have taken pressure levels corresponding to the measurement
37 location of GOSAT/TANSO-FTS TIR data shown in the figure.
38

1 *Fig.4: Please replace “Altitude [km] in Y axis label with “Pressure [hPa]”.*

2
3 Reply:

4 We have corrected the label of the vertical axis (y-axis) of Figure 4 of the revised manuscript. We
5 appreciate you pointing out our mistake.

6
7 *Fig.7: I think drawing zero lines (i.e. no bias) in each panel makes the bias correction validity more*
8 *visible.*

9
10 Reply:

11 Following your advice, we have drawn zero lines in each of the four panels of Figure 7 of the
12 revised manuscript. We have also drawn zero lines in Figure 8 and 9 to show differences between
13 each histogram clearly. We appreciate your suggestion.

14
15 *Fig.7 caption “Thick and dashed lines indicate the biases of the original TIR CO₂ data (no bias*
16 *correction) and bias-corrected TIR CO₂ data, respectively.”:*

17 *1. On my screen, all lines in each panel seem to have same line thickness. Do the authors mean “solid*
18 *and dashed lines”?*

19 *2. This sentence does not match the main text which says that thick lines are bias-corrected values.*

20
21 Reply:

22 We appreciate you pointing out our mistake.

23 1. We have replaced “thick lines” with “solid lines” and exchanged “solid” for “dashed” in the
24 caption for Figure 7 of the revised manuscript as follows:

25 “Dashed and solid lines indicate the biases of the original TIR CO₂ data (no bias correction) and
26 bias-corrected TIR CO₂ data, respectively.”

27 2. We have replaced “thick lines” with “solid lines” in the sentences related to Figure 7 in the
28 revised manuscript.

29
30 *Fig.11, gray shade: Could the authors explain what gray zones in the figure are? (No data or out of*
31 *color scale?)*

32
33 Reply:

34 Gray color in Figure 11 means no GOSAT/TANSO-FTS TIR CO₂ data in a 2.5° grid area.
35 Following your advice, we have explained the meaning of gray color in the caption for Figure 11
36 of the revised manuscript as follows:

37 “There are no GOSAT/TANSO-FTS TIR CO₂ data in gray-shaded areas.”

1 **Reply to Referee #2,**

2

3 *Overall, this is a good paper dealing with difficult but necessary bias corrections to TANSO-FTS*
4 *observations of mid-troposphere CO₂. It's a tricky subject, but the methodology is generally sound. However,*
5 *the paper is difficult to follow in some sections, and in many cases, the figures need some improvement and*
6 *clarification. I would recommend publication after some revisions in the text, and if the authors could better*
7 *address the issue of the number of layers in the forward model (see comment for page 10, line 32 below.)*

8

9 *General comment: Throughout the paper, the authors refer to the retrieval layers by number (layer 3, layer*
10 *4, etc.), rather than, say, its log mean pressure. These layer numbers are specific to their algorithm, and*
11 *referencing the layers by number is a little burdensome to the reader, even where the pressures are provided.*
12 *For example, Page 6, line 23 reads "Saitoh et al. (2016) showed that TIR V1 CO₂ data agreed well with*
13 *CME level flight CO₂ data in the UT region corresponding to retrieval layers 9 and 10." This would read*
14 *better if the pressures were given instead of the layer numbers. I suggest they prepare a table listing the*
15 *retrieval layer numbers, layer boundary pressures, and the log-mean pressures of the layers (similar to*
16 *Table 1 of Saitoh et al., 2016), and then just refer to a layer by its mean pressure rather than its number.*

17

18 Reply:

19 We greatly appreciate your comments. As described above, we have added Table 1 to show
20 representative pressure levels of each of the retrieval grid layers used in the
21 GOSAT/TANSO-FTS TIR V1 L2 CO₂ retrieval processing and referred to the retrieval grid
22 layers by the representative pressure levels instead of retrieval grid numbers. In Table 1, we have
23 kept the retrieval grid numbers for the convenience of TIR CO₂ data users. In the TIR V1 L2 CO₂
24 retrieval algorithm, we have calculated representative pressure level P_{r_{lay}}, which is
25 thermodynamically mean pressure level, by the following expression [Gallery et al., 1983]:

$$P_{\text{rlay}} = \left\{ \frac{H_p H_p}{H_p + H_p} (P_{\text{rlev}_j} \rho_{\text{rlev}_j} - P_{\text{rlev}_{j+1}} \rho_{\text{rlev}_{j+1}}) \right\} / \{ H_p (\rho_{\text{rlev}_j} - \rho_{\text{rlev}_{j+1}}) \}$$

$$H_p = \frac{-\Delta z}{\log_e (P_{\text{rlev}_{j+1}} / P_{\text{rlev}_j})}$$

26

$$H_p = \frac{-\Delta z}{\log_e (\rho_{\text{rlev}_{j+1}} / \rho_{\text{rlev}_j})}$$

$$\Delta z = \log_e \frac{P_{\text{rlev}_{j+1}}}{P_{\text{rlev}_j}} \times -\frac{Rd}{g} \times \frac{|T_{\text{rlev}_{j+1}} - T_{\text{rlev}_j}|}{2}$$

27 where P_{r_{lev}_j} and P_{r_{lev}_j+1} are lower and upper pressure levels of each retrieval grid layer,
28 respectively, T_{r_{lev}_j} and T_{r_{lev}_j+1} are temperatures at the two pressure levels, ρ_{r_{lev}_j} and ρ_{r_{lev}_j+1} are
29 air densities at the two pressure levels, Rd is the gas constant, and g is the acceleration of gravity.
30 Representative pressure levels change depending on temperature, which are stored in each of the

1 TIR V1 L2 CO₂ data files, but their variabilities are quite small. In Table 1, we have presented
2 the averages of representative pressure levels of each retrieval grid layer calculated by using all
3 GOSAT/TANSO-FTS measurements in 2010.

4
5 *Page 1, line 14: "...good spatial representability." It's not obvious what 'representability' means here.*
6 *Would "resolution and precision" be a better phrase to use?*

7
8 Reply:

9 CO₂ concentrations in the free troposphere are well mixed compared to the concentrations near
10 the surface and less affected by local point sources of CO₂; in that context, observations in the
11 free troposphere can obtain CO₂ concentrations representative of regions, which can be dealt with
12 in a global model estimating CO₂ surface fluxes. In the revised manuscript, we have modified the
13 sentence to clarify this point as follows:

14 "CO₂ observations in the free troposphere can be useful for constraining CO₂ source and sink
15 estimates at the surface due to their representativeness being away from local point sources of
16 CO₂."

17
18 *Page 1, line 24: "(retrieval layers 5–6), ..." It's not necessary to get into the details of their retrieval*
19 *method in the abstract.*

20
21 Reply:

22 We have deleted the phrase in the abstract of the revised manuscript following your advice.

23
24 *Page 2, line 3: Suggest changing "(e.g., Gurney et al., 2002 Gurney et al., 2004)" to "(e.g., Gurney et al.,*
25 *2002; 2004)".*

26
27 Reply:

28 Following your suggestion, we have modified the text in how to cite the references.

29
30 *Page 2, line 24: "spatial representability." Again, not obvious what it means here.*

31
32 Reply:

33 XCO₂ data obtained by measurements utilizing short-wave infrared (SWIR) band contained
34 information on CO₂ concentrations near the surface compared to free tropospheric CO₂
35 measurements utilizing TIR band. However, satellite-borne sensors have relatively large
36 field-of-views, and therefore their XCO₂ data are averaged concentrations in their field of views
37 of several kilometers that are not too much affected by strong local point sources of CO₂. In the
38 revised manuscript, we have modified the sentence as follows:

1 “Global XCO₂ data based on satellite observations are averaged concentrations in their field of
2 views of several kilometers that are not too much affected by strong local point sources of CO₂,
3 and have therefore been used to estimate surface CO₂ fluxes (Maksyutov et al., 2013; Saeki et al.,
4 2013a; Chevallier et al., 2014; Basu et al., 2013, 2014; Takagi et al., 2014).”

5
6 *Page 3, line 16: Suggest changing “...and has continued CO₂ and CH₄ operational measurements for*
7 *approximately eight years.” to “and has continued operational measurements of CO₂ and CH₄ for*
8 *approximately eight years.*

9
10 Reply:

11 Following your suggestion, we have modified the sentence.

12
13 *Page 3, line 23: Suggest shortening “These studies showed the following: 1) TIR UT CO₂ data agreed...” to*
14 *“These studies showed: 1) TIR UT CO₂ data agreed...”*

15
16 Reply:

17 Following your suggestion, we have modified the sentence.

18
19 *Page 5, line 14: Suggest more explanation of why the averaging kernels are applied to the CME data and*
20 *then comparison made. This would be useful to the reader not well versed in averaging kernels etc.*

21
22 Reply:

23 Following your advice, we have added more explanation of why we should apply TIR CO₂
24 averaging kernel functions to CME aircraft profiles as follows:

25 “Observations by satellite-borne nadir-viewing sensors like TANSO-FTS have much lower
26 vertical resolution than aircraft observations. Therefore, we smoothed the CME_obs. profile to fit
27 its vertical resolution to the vertical resolution of corresponding TIR CO₂ profile by applying TIR
28 CO₂ averaging kernel functions (AK) to the CME_obs. profile, as follows (Rodgers and Connor,
29 2003):”

30
31 *Page 6, Section 4.2: It’s not obvious why an “average” averaging kernel can be applied and not sometimes*
32 *be misleading. In addition to the effect of instrument parameters (SNR, spectral resolution, view angle etc.)*
33 *and assuming clear scenes only, the averaging kernel could vary by temperature gradient and thermal*
34 *contrast with the surface. How much does an averaging kernel vary within a grid box? It would help if the*
35 *authors briefly explain why they’re using an averaged AK here and discuss the limitations of doing so.*

36
37 Reply:

38 We agree with you. TIR CO₂ averaging kernel functions depend on TIR measurement spectral

1 noise, a priori CO₂ profile variability, and CO₂ Jacobians. In the TIR V1 L2 CO₂ retrieval
2 algorithm, we set covariance matrices of the TIR measurement noise and a priori CO₂ profile in
3 the same manner for all TIR CO₂ measurements, as described in Saitoh et al. (2016). The CO₂
4 Jacobians depend on temperature and CO₂ profiles, and therefore change with location and time.
5 For a validation purpose based on one-by-one comparisons like TIR versus CME CO₂ profiles,
6 we should apply corresponding TIR CO₂ averaging kernel functions, not averaged one. On the
7 other hand, the purpose of comparisons between TIR and NICAM-TM CO₂ data is to evaluate the
8 bias-correction values determined for each vertical layer, latitude band, and season. In addition,
9 TIR CO₂ averaging kernel functions showed nearly identical structures with each other when
10 collected for each 2.5° grid in one month, which means that applying the monthly averaged TIR
11 CO₂ averaging kernel functions did not affect the conclusions of this study. From this standpoint,
12 using monthly averaged TIR CO₂ averaging kernel functions instead of individual one is enough
13 for our purpose. In the revised manuscript, we have added one paragraph in Section 4.2 and
14 discussed the effect of using monthly averaged TIR CO₂ averaging kernel functions on our
15 analysis. We appreciate your comments.

16
17 *Page 7, line 14 “In addition, negative biases of TIR CO₂ data against NICAM-TM CO₂ data increased by 1*
18 *ppm or less per year in all seasons, judging from the mode values, although the increase in negative biases*
19 *was not evident in the comparisons over airports shown in Figure 6.” I did not quite understand what is*
20 *meant by this. Do they mean the bias varied by 1ppm or less?*

21
22 Reply:

23 We intended to say the following: negative biases of TIR CO₂ data against NICAM-TM CO₂ data
24 seemed to increase over time, judging from each of the mode values for the three years and the
25 rate of the increase was around and less than 1 ppm; however, the increase in the negative biases
26 against NICAM-TM CO₂ data was not evident as was the case with the negative biases against
27 CME CO₂ data discussed in Section 5.1. In the revised manuscript, we have modified the
28 sentence as follows:

29 “In addition, negative biases of TIR CO₂ data against NICAM-TM CO₂ data in all seasons
30 slightly increased over time, judging from the mode values, although the increase in negative
31 biases was not much evident as in the comparisons over airports shown in Figure 6.”

32
33 *Page 8, line 27: Typo: “... in the LT and ML regions.” Did they mean “MT” regions?*

34
35 Reply:

36 We have modified the sentence. We appreciate you pointing out our mistake.

37
38 *Page 9, line 13: “As shown in Figure 6, the largest negative biases in TIR V1 CO₂ data existed in the MT*

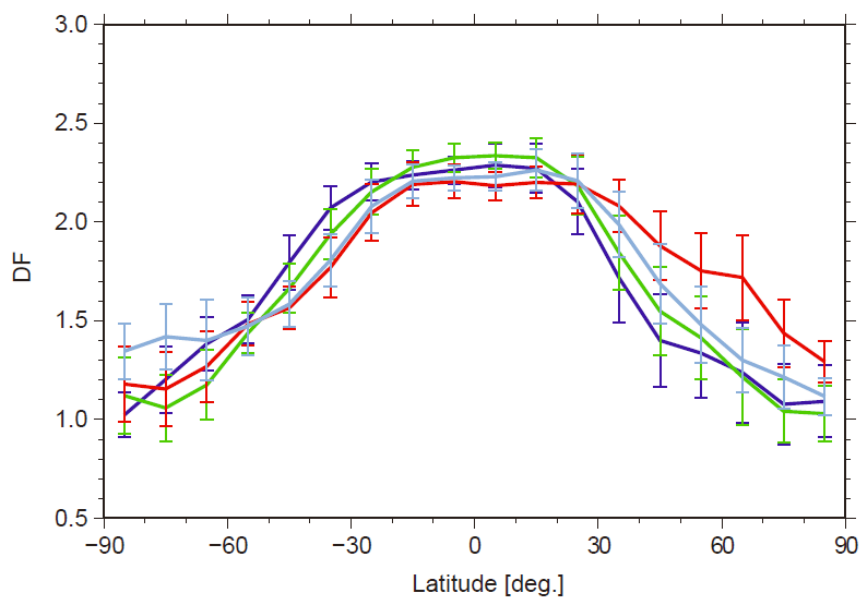
1 region in middle and low latitudes during spring and summer, where TANSO-FTS TIR measurements have
2 relatively large sensitivity to CO₂ concentrations and thus the retrievals are less constrained to a priori
3 concentrations.” Some kind of comparison is in order to quantify the difference in CO₂ sensitivity here – say
4 average row-sum of averaging kernels, or total DOFS as a function of latitude.

5
6 Reply:

7 We totally agree with you. We have modified the related sentences for consistency with the
8 sentences in the second paragraph of Section 5.1, and then provided information on degrees of
9 freedom of TIR V1 CO₂ data in low latitudes where the largest negative biases existed:

10 “As shown in Figure 6, the largest negative biases in TIR V1 CO₂ data existed in the MT region
11 in low latitudes (20°S–20°N) during the JJA season. Degrees of freedom (DF) of TIR V1 CO₂
12 data were highest in low latitudes, exceeding 2.2 in all seasons, which means retrieved CO₂
13 concentrations there contained more information coming from TANSO-FTS TIR L1B spectra and
14 thus were relatively less constrained to a priori concentrations.”

15 The DF values have been referred from the below figure that shows monthly averaged DF values
16 for each 10° latitude in January (blue), April (green), July (red), and October (light blue) in 2010.



18 Reference figure. Monthly averaged DF values of TIR V1 CO₂ data for each 10° latitude in
19 January, April, July, and October 2010, shown by blue, green, red, and light blue lines,
20 respectively. Here, GOSAT/TANSO-FTS observations with high elevated areas (surface
21 pressure less than 736 hPa) were excluded.

22
23
24 Page 9, line 15: “This implies that biases in L1B spectra are a major cause of the negative biases in
25 retrieved CO₂ concentrations, as Saitoh et al. (2016) noted in the UT region.” The wording is confusing.
26 Does this mean there are biases in the L1b radiances related to latitude and season, or are there fitting
27 biases from the retrieval algorithm? Judging from the rest of the paragraph where the authors write about

1 *retrieval of surface parameters, I think they're referring to fitting bias, but whatever the bias is, it should be*
2 *explicitly described.*

3
4 Reply:

5 According to comparisons between TANSO-FTS TIR and S-HIS radiance spectra (Kataoka et al.,
6 2014) and theoretical radiance error estimations (Kuze et al., 2016), TANSO-FTS TIR L1B
7 radiance spectra had considerable biases. In low latitudes, retrieved CO₂ data contained more
8 information coming from TANSO-FTS TIR L1B spectra judging from their highest DF values.
9 This means that the effect of the L1B radiance biases should be also largest in TIR CO₂ data in
10 low latitudes. The magnitude of the TIR L1B radiance biases may change by scene, but we have
11 not yet drawn any conclusion on the dependence of the radiance biases on time, location, viewing
12 angle, thermal condition of TANSO-FTS instrument, and so on. As the related three paragraphs
13 in Discussion were less organized, we have reorganized the discussion on the relation between
14 L1B radiance biases and L2 CO₂ negative biases against CME CO₂ data in the revised
15 manuscript.

16
17 *Page 10, line 4: "From these results, we conclude that using the 10- μ m band in conjunction with the 15- μ m*
18 *and 9- μ m bands in the VI retrieval algorithm is a probable cause of the negative biases in retrieved CO₂*
19 *concentrations in the LT and MT regions." While I don't disagree with this, this would be more convincing if*
20 *the authors compared their results using the different mixes of CO₂ bands directly against the aircraft*
21 *measurements.*

22
23 Reply:

24 We totally agree with you. We have also showed nearby CME CO₂ profiles by gray lines in
25 Figure 10 of the revised manuscript other than TIR CO₂ retrieval results. We appreciate your
26 suggestion.

27
28 *Page 10, Line 13: "According to Figure 13 in Kuze et al. (2016), there was no distinct uncertainty in the*
29 *10- μ m band in the latest version of the TANSO-FTS TIR spectra." The wording of this leaves me uncertain*
30 *of what they're claiming. Uncertainty of linestrengths or low fitting residual? Are they saying that using the*
31 *10 micron band of CO₂ does not add significant bias? This should be clarified.*

32
33 Reply:

34 Kuze et al. (2016) performed theoretical estimation of radiance biases of TANSO-FTS TIR L1B
35 V161 and newer version V201 spectra. The radiance biases inherent in the TANSO-FTS TIR
36 L1B spectra were attributable to several calibration issues, mainly due to polarization correction.
37 According to theoretical calculations shown in Figure 13 in Kuze et al. (2016), there were no
38 distinct radiance biases in the 10- μ m band (930–990 cm⁻¹) in the latest version of the

1 TANSO-FTS TIR spectra. If it is true for observed TIR radiances, our test retrievals imply that
2 simultaneous retrieval of surface parameters for TIR spectra at the 10- μ m band with less radiance
3 bias worsened CO₂ retrieval results. We have clearly stated this in the revised manuscript.
4

5 *Page 10, paragraph beginning line 17: As noted earlier, it would really help the reader if the authors*
6 *referred to the retrieval layers by pressure and not layer number.*
7

8 Reply:

9 Following your advice, we have referred to the lower and upper pressure levels of the two
10 retrieval grid layers that we focused on.
11

12 *Page 10, line 32: "In retrieval from TIR spectra, the more atmospheric layers in which we retrieve CO₂*
13 *concentrations, the lower the information content of the retrieval result in each layer becomes; as a result,*
14 *the retrieved concentrations are constrained by a priori model data. Thus, there is a high possibility of large*
15 *biases in retrieved TIR CO₂ concentrations in low latitudes." This assertion needs to be tested. It is true that*
16 *with more layers, the information is spread out more, but the overall information content, as measured by*
17 *the degrees-of-freedom-of-signal (trace of the averaging kernel) can be the same or very similar, as can the*
18 *retrieved profiles (depending on what the off-diagonals are for the a priori background covariance.) It's*
19 *quite possible that if the background a priori is biased, then a TIR retrieval can also be biased not because*
20 *of the number of retrieval layers, but, particularly at low latitudes, because of water vapor interference,*
21 *undetected boundary- layer clouds changing the thermal contrast with the surface, or biases in the*
22 *temperature. Again, this needs to be tested, or the statement removed or at least reworded as a*
23 *hypothesizing.*
24

25 Reply:

26 We totally agree with you. Our wording in the original manuscript leads to misunderstanding. We
27 here intended to say that TIR CO₂ retrieval were somewhat constrained by a priori concentrations.
28 In the MT region in low latitudes, a priori CO₂ concentrations taken from the NIES-TM05 model
29 probably have larger uncertainties due to the parameterization of vertical transport. Therefore,
30 there is a possibility of more biases attributed to the a priori uncertainties in retrieved TIR CO₂
31 data there. Following your suggestion, we have removed the related statement and modified the
32 sentences in the revised manuscript as follows:

33 "In low latitudes, there are relatively strong updrafts, and thus there are larger uncertainties
34 among models than in other areas due to differences in the parameterization of vertical transport.
35 Therefore, a priori CO₂ concentrations taken from the NIES-TM05 model (Saeki et al., 2013b)
36 probably have larger uncertainties in the MT region in low latitudes. As retrieved TIR CO₂
37 concentrations were to some extent constrained by a priori concentrations, they possibly had
38 more biases attributed to the a priori uncertainties in the MT region in low latitudes."

1 We greatly appreciate your comment.

2
3 *Figure 5: It would be much clearer to the reader if they provided guidance to the different panels and lines*
4 *in a legend box on the figure, rather than only in the caption. It would also help, for a reader skimming the*
5 *paper, to describe what “CME_AK CO₂” means in the caption as well as the text of the paper.*

6
7 Reply:

8 Following your advice, we have provided information on seasons in each panel and described
9 each line in both left and right sides of the panel (a). In the caption of the revised manuscript, we
10 have described what CME_AK CO₂ means as follows:

11 “The CME_AK CO₂ data are CME CO₂ data to which TIR CO₂ averaging kernel functions are
12 applied.”

13
14 *Figure 6: Use pressures and not layer numbers on vertical axis. It would also be better if latitude*
15 *information and season (line color) were provided as a legend on the figure. It would help if the lines in the*
16 *top panels had slight vertical offsets to clarify how different the error bars are from each other.*

17
18 Reply:

19 Following your advice, we have presented the representative pressure levels of the six retrieval
20 grid layers shown in Table 1 instead of their layer numbers. We have provided information on
21 latitude bands and colors for seasons as a legend and slightly shifted horizontal bars for 1- σ
22 standard deviations in Figure 6 of the revised manuscript. We appreciate your comments.

23
24 *Figure 7: It’s not clear here (or in the text) at what pressures they are comparing avg CO₂ with NICAM. The*
25 *contrast between the mid-gray and light-gray lines is not enough to easily distinguish between them.*

26
27 Reply:

28 Figure 7 includes all comparison results between TIR and NICAM-TM CO₂ data in the six
29 retrieval grid layers from 736 to 287 hPa (retrieval layers 3–8). In the revised manuscript, we
30 have stated this clearly in the revised manuscript as follows:

31 “Figure 7 shows the frequency distributions of differences in monthly averaged CO₂
32 concentrations between TIR and NICAM-TM CO₂ data in all retrieval layers from 736 to 287
33 hPa in all 2.5° grids over the latitude range of 40°S to 60°N.”

34 Following your advice, we have presented the lower and upper pressure levels of the six retrieval
35 layers that we focused on and used red and blue colors instead of light-gray and mid-gray colors
36 in Figure 7 of the revised manuscript. We appreciate your comments.

37
38 *Figure 8: Please use pressures instead of layer numbers. Again, the contrast between the mid-gray and*

1 *light-gray lines is not enough to easily distinguish between them.*

2
3 Reply:

4 Following your advice, we have presented the lower and upper pressure levels of each set of the
5 six retrieval grid layers that we focused on and used red and blue colors instead of light-gray and
6 mid-gray colors in Figure 8 of the revised manuscript.

7
8 *Figure 9: Again, please state the pressures instead of “layer 7-8.”*

9
10 Reply:

11 Following your advice, we have modified Figure 9 to present the lower and upper pressure levels
12 of the two retrieval grid layers that we focused on.

13
14 *Figure 10: Please also describe the lines and the location/times the different panels represent as a legend*
15 *rather than just in the caption.*

16
17 Reply:

18 Following your advice, we have modified Figure 10: we have separated the two results of Figure
19 10(b) and discarded the result of Figure 10(a) of the original manuscript to simplify the figure,
20 provided information on the locations (both over Narita airport) and dates ((a) April 1, 2010 and
21 (b) April 30, 2010) of the two results in the caption and each of the panels, and described each of
22 the five lines in the panel (b).

23
24
25 In the revised manuscript showing the changes made that is attached below, we have showed the
26 changes that we made to address the comments by Referee #1 by blue color, and the changes that we
27 had made to address the comments by Referee #2 and have been already reflected in AMTD by red
28 color.

Bias assessment of lower and middle tropospheric CO₂ concentrations of GOSAT/TANSO-FTS TIR Version 1 product

Naoko Saitoh¹, Shuhei Kimoto^{1*}, Ryo Sugimura^{1**}, Ryoichi Imasu², Kei Shiomi³, Akihiko Kuze³,
Yousuke Niwa⁴, Toshinobu Machida⁵, Yousuke Sawa⁴, and Hidekazu Matsueda⁴

5 ¹Center for Environmental Remote Sensing, Chiba University, Chiba, 263-8522, Japan

²Atmosphere and Ocean Research Institute, The University of Tokyo, Kashiwa, 277-8564, Japan

³Japan Aerospace Exploration Agency, Tsukuba, 305-8505, Japan

⁴Meteorological Research Institute, Tsukuba, 305-0052, Japan

⁵National Institute for Environmental Studies, Tsukuba, 305-8506, Japan

10 *Now at the Japan Research Institute, Tokyo, 141-0022, Japan

**Now at Fujitsu FIP Corporation, Tokyo, 105-8668, Japan

Correspondence to: Naoko Saitoh (nsaitoh@faculty.chiba-u.jp)

Abstract. CO₂ observations in the free troposphere can be useful for constraining CO₂ source and sink estimates at the surface due to their ~~good spatial~~ representativeness being away from local point sources of CO₂ ~~ability~~. The thermal infrared (TIR) band of the Thermal and Near Infrared Sensor for Carbon Observation (TANSO)–Fourier Transform Spectrometer (FTS) on board the Greenhouse Gases Observing Satellite (GOSAT) has been observing global CO₂ concentrations in the free troposphere for about 8 years, and thus could provide a dataset with which to evaluate the vertical transport of CO₂ from the surface to the upper atmosphere. This study evaluated biases in the TIR version 1 (V1) CO₂ product in the lower troposphere (LT) and the middle troposphere (MT) (736–287 hPa), on the basis of comparisons with CO₂ profiles obtained over airports using Continuous CO₂ Measuring Equipment (CME) in the Comprehensive Observation Network for Trace gases by AirLiner (CONTRAIL) project. Bias-correction values are presented for TIR CO₂ data for each pressure layer in the LT and MT regions during each season and in each latitude band: 40°S–20°S, 20°S–20°N, 20°N–40°N, and 40°N–60°N. TIR V1 CO₂ data had consistent negative biases of 1–1.5% compared with CME CO₂ data in the LT and MT regions, with the largest negative biases at 541–398 hPa (~~retrieval layers 5–6~~, ~~especially in low latitudes during northern summer (up to~~ 25 ~~7.3 ppm)~~, ~~partly likely~~ due to the use of ~~spectra at a~~ 10- μ m CO₂ absorption band in conjunction with 15- μ m and 9- μ m absorption bands in the V1 retrieval algorithm. Global comparisons between TIR CO₂ data to which the bias-correction values ~~were had been~~ applied and CO₂ data simulated by Nonhydrostatic ICosahedral Atmospheric Model (NICAM)-based transport model (TM) confirmed the validity of the bias-correction values evaluated over airports in limited areas. In low latitudes in the upper MT region (398–287 hPa), however, TIR CO₂ data in northern summer were overcorrected by these 30 bias-correction values; this is because the bias-correction values were determined using comparisons mainly over airports in SouthEast Asia where CO₂ concentrations in the upper atmosphere display relatively large variations due to strong updrafts.

1. Introduction

CO₂ in the atmosphere is the most influential greenhouse gas (IPCC, 2013 and references therein). Many studies have been conducted to estimate the sources and sinks of atmospheric CO₂ using both observational data and transport models (e.g., Gurney et al., 2002; ~~Gurney et al., 2004~~). In CO₂ inversion studies, accurate atmospheric CO₂ observations with ~~good~~ spatial representativeness are desirable, which can be obtained from elevated sites such as tall towers and mountains or over the ocean. Patra et al. (2006) demonstrated the robustness of CO₂ surface flux estimation using CO₂ data obtained solely from ocean sites compared to data obtained from both ocean and land sites; this was because the models discussed therein were unable to successfully simulate CO₂ data over land, as these sites were more affected by local point sources of CO₂.

Uncertainties in atmospheric transport processes also result in differences in CO₂ surface fluxes estimated by inverse models.

CO₂ is chemically inactive, and thus long-range transport processes as well as surface fluxes determine its horizontal distribution and seasonal cycle in the atmosphere (Miyazaki et al., 2008; Barnes et al., 2016). The treatment of vertical transport of CO₂ also produces differences in simulated CO₂ concentrations in the free troposphere among transport models unrelated to surface fluxes (Niwa et al., 2011a). Therefore, it is needed to observe CO₂ concentrations over land that are not strongly affected by local point sources of CO₂ emissions, as well as CO₂ concentrations in the free troposphere that can evaluate vertical CO₂ transport from the surface in transport models.

Satellite-borne nadir-viewing sensors can observe averaged CO₂ concentrations, with horizontal resolution ranging from several kilometers to tens of kilometers. Column-averaged dry-air mole fractions of CO₂ (XCO₂) have been observed utilizing CO₂ absorption bands in the shortwave infrared (SWIR) regions at around 1.6 and/or 2.0 μm by satellite-borne sensors such as the Scanning Imaging Absorption Spectrometer for Atmospheric Chartography (SCIAMACHY) on the Environmental Satellite (ENVISAT) (Buchwitz et al., 2005; Barkley et al., 2006), the Thermal and Near Infrared Sensor for Carbon Observation (TANSO)–Fourier Transform Spectrometer (FTS) on the Greenhouse Gases Observing Satellite (GOSAT) (Yoshida et al., 2011, 2013; O’Dell et al., 2012; Butz et al., 2011; Cogan et al., 2012), and the Orbiting Carbon Observatory 2 (OCO-2) (Crisp et al., 2017; Connor et al., 2016). Global XCO₂ data based on satellite observations are

averaged concentrations in their field of views of several kilometers that are not too much affected by strong local point sources of CO₂ have relatively good spatial representability, and have therefore been used to estimate surface CO₂ fluxes (Maksyutov et al., 2013; Saeki et al., 2013a; Chevallier et al., 2014; Basu et al., 2013, 2014; Takagi et al., 2014). CO₂ concentrations in the free troposphere can be obtained by satellite-borne sensors with thermal infrared (TIR) bands at around 4.6, 10, and/or 15 μm, provided by the following sensors: the High-Resolution Infrared Sounder (HIRS) (Chédin et al., 2002, 2003, 2005), the Interferometric Monitor for Greenhouse Gases (IMG) (Ota and Imasu, 2016), the Atmospheric Infrared Sounder (AIRS) (Crevoisier et al., 2004; Chahine et al., 2005; Maddy et al., 2008; Strow and Hannon, 2008), the Tropospheric Emission Spectrometer (TES) (Kulawik et al., 2010, 2013), the Infrared Atmospheric Sounding Interferometer (IASI) (Crevoisier et al., 2009), and the TANSO-FTS (Saitoh et al., 2009, 2016). Furthermore, CO₂ concentrations in several atmospheric layers within the free troposphere can be retrieved separately from high-resolution TIR spectra (Saitoh et al.,

2009; Kulawik et al., 2013). Such vertical CO₂ data offer a good constraint for CO₂ surface flux estimates (Kulawik et al., 2010), and have the potential to evaluate the vertical transport of CO₂ from the surface to the upper atmosphere, if they have sufficient accuracy.

5 Previously, the data quality of CO₂ product from the GOSAT/TANSO-FTS TIR band has been examined in the upper troposphere and the lower stratosphere (UTLS) region, where TIR observations have the most sensitivity to CO₂ concentrations. Saitoh et al. (2016) evaluated biases in UTLS (287–162 hPa) CO₂ data of TIR version 1 (V1) Level 2 (L2) product for the year 2010 through comparisons with UTLS CO₂ data collected with broad spatial coverage by Continuous CO₂ Measuring Equipment (CME) in the Comprehensive Observation Network for Trace gases by AirLiner (CONTRAIL) project. ~~We evaluated the biases, growth rates, and seasonal variations in the TIR V1 UT CO₂ data for three years, from 2010 to 2012 (Saitoh et al., 2017).~~
10 In this study, we validated the TIR V1 CO₂ product in the lower troposphere (LT) and the middle troposphere (MT) (736–287 hPa) by comparing them with CONTRAIL CME CO₂ profiles over airports, and calculated bias-correction values for the TIR CO₂ data, based on comparisons by latitude, pressure layer, and season from 2010 to 2012. We then examined the validity of the bias-correction values evaluated in limited areas over airports by comparing TIR CO₂ data before and after applying the bias-correction values to CO₂ data simulated using Nonhydrostatic
15 ICosahedral Atmospheric Model (NICAM)-based transport model (TM) (Niwa et al., 2011b).

2. GOSAT/TANSO-FTS and CONTRAIL CME observations

GOSAT, launched on 23 January 2009, and has continued operational measurements of CO₂ and CH₄ ~~operational measurements~~ for approximately eight years. TANSO-FTS on board GOSAT consists of three bands in the SWIR region and one in the TIR region (Kuze et al., 2009). The TIR band of TANSO-FTS makes observations both in daytime and nighttime, unlike the SWIR band.
20 We analyzed the latest CO₂ product from the TIR band of TANSO-FTS, the TIR V1 L2 CO₂ product. The TIR V1 L2 CO₂ product was generated from TANSO-FTS version 161.160 (V161) Level 1B (L1B) radiance spectra. Saitoh et al. (2016) described the retrieval algorithm for the TIR V1 L2 CO₂ product in detail. In the TIR V1 L2 algorithm, CO₂ concentrations are retrieved in 28 vertical grid layers from the surface to 0.1 hPa. Saitoh et al. (2016) and Saitoh et al. (2017) evaluated biases in TIR V1 CO₂ data in the UTLS region ~~corresponding to retrieval layers 9–11~~ (287–162 hPa) and
25 calculated growth rates and amplitudes of seasonal variations in TIR V1 UT CO₂ data. These studies showed ~~the following~~:
1) TIR UT CO₂ data agreed with CME CO₂ data to within 0.1% and an average of 0.5% in the Southern and Northern Hemispheres, respectively; 2) these data exhibited negative biases larger than 2 ppm in spring and summer in northern low and middle latitudes; 3) their negative biases increased over time partly due to constraint by a priori data with low growth rates taken from National Institute for Environmental Studies (NIES) transport model, NIES-TM05 (Saeki et al., 2013b); and
30 4) they displayed more realistic seasonal variations in UT CO₂ concentrations than a priori data. In this study, we validated the quality of TIR V1 CO₂ data in the LT (736–541 hPa) and MT (541–287 hPa) regions, ~~defined as retrieval layers 3–4~~

~~(736–541 hPa) and 5–8 (541–287 hPa), respectively~~, by comparing them to CONTRAIL CME CO₂ data. Table 1 shows pressure levels of retrieval grid layers of the TIR V1 CO₂ product that this study focused on.

CONTRAIL is a project to observe atmospheric trace gases, such as CO₂ and CH₄, using two types of instruments installed on commercial aircraft operated by Japan Airlines (JAL) starting in 2005. Of the two instruments, CME can observe CO₂ concentrations more frequently over a wide area (Machida et al., 2008). See Machida et al. (2008) and Machida et al. (2011) for details about CME CO₂ observations. This study used CO₂ data obtained with CME during the ascent and descent flights over several airports from 2010 to 2012. Figure 1 shows the locations of the airports used here, which fall in the latitude range of 40°S to 60°N.

3. NICAM-TM CO₂ data

We used atmospheric CO₂ data simulated by NICAM-TM (Niwa et al., 2011b) for global comparison with TANSO-FTS TIR CO₂ data. NICAM has quasi-homogeneous grids, with horizontal grids generated by recursively dividing an icosahedron. The NICAM simulations used in this study were performed with a horizontal resolution of around 240 km, which corresponds to the horizontal resolution when an icosahedron is divided five times (“glevel-5”). See Tomita and Satoh (2004) and Satoh et al. (2008, 2014) for details of NICAM. The transport model version of NICAM, NICAM-TM, has been developed and used for atmospheric transport and source/sink inversion studies of long lived species such as CO₂ (Niwa et al., 2011a,b, 2012, 2017).

In this study, simulation of NICAM-TM used inter-annually varying flux data of fossil fuel emissions (Andres et al., 2013) and biomass burnings (van der Werf et al., 2010), and the residual natural fluxes from the inversion of Niwa et al. (2012), which mostly represent fluxes from the terrestrial biosphere and oceans. The inversion analysis of Niwa et al. (2012) was performed for 2006–2008 and the three-year-mean fluxes were used in this study. In the inversion analysis, CONTRAIL CO₂ data obtained during ascending, descending, and cruise level flights were categorized into four vertical bins: 575–625, 475–525, 375–425, and 225–275 hPa, and the binned CONTRAIL CO₂ data were then~~The NICAM TM CO₂ data used here incorporated CONTRAIL CO₂ data into the inverse model, in addition to surface CO₂ data (Niwa et al., 2012). CONTRAIL CO₂ data obtained during ascending, descending, and cruise level flights were categorized into four vertical bins: 575–625, 475–525, 375–425, and 225–275 hPa. The binned CONTRAIL CO₂ data were then incorporated into NICAM TM inversion calculations to estimate surface CO₂ fluxes.~~ Niwa et al. (2012) showed that incorporating the CONTRAIL CO₂ data into the surface flux inversion model improved CO₂ concentration simulation compared with a simulation using surface CO₂ data only. They also demonstrated that the simulated CO₂ concentrations based on CONTRAIL CO₂ data showed better agreement with independent upper atmospheric CO₂ data obtained in the Civil Aircraft for the Regular Investigation of the atmosphere Based on an Instrument Container (CARIBIC) project (Brenninkmeijer et al., 2007). Furthermore, the CO₂ forward simulation of NICAM-TM for 2010–2012 showed a good agreement with in-situ CO₂ observations not only in seasonal cycles but also in trends in spite of using the fluxes optimized for 2006–2008; the simulated growth rate at the

[Minamitorishima station \(e.g., Wada et al., 2011\)](#), which is one of the [global stations of the Global Atmospheric Watch \(GAW\)](#), was 2.4 ppm/yr for 2010–2012, while the growth rate based on in-situ observations was 2.2 ppm/yr.

4. Methods

4.1 Bias assessment of TIR CO₂ data using CME observations

5 Vertical distribution of CO₂ concentrations can be obtained by CME during the ascent flights from departure airports and the descent flights to destination airports. Figure 2 shows the flight tracks of CME ascending and descending observations over Narita airport, [Japan \(35.8°N, 140.4°E\)](#) in 2010. CME CO₂ data were regarded as part of the CO₂ vertical profiles, with maximum altitudes around 12 km, and were obtained within 3–4° of latitude and longitude of the airport. Therefore, we set the threshold for selecting coincident pairs of TANSO-FTS TIR and CME CO₂ profiles for comparison to be a 300-km
10 distance from each of the airports shown in Figure 1.

For each of the coincident pairs, we calculated the weighted average of discrete CME CO₂ data in a vertical layer, “CME_raw”, represented by black circles in Figure 3(a), with respect to the center pressure levels of each of the 28 vertical grid layers of TIR CO₂ data. When there were no corresponding CME CO₂ data in lower retrieval grid layers, CO₂ concentration at the lowest altitude observed by CME was assumed to be constant down to the lowest retrieval grid layer.

15 Similarly, the uppermost CO₂ concentration observed was assumed to be constant up to the center pressure level of the retrieval grid layer including the tropopause, identified based on temperature lapse rates of Global Spectral Model Grid Point Values from the Japan Meteorological Agency (JMA-GPV) interpolated to the location of CME measurement. In retrieval grid layers above the tropopause, CO₂ concentrations were determined based on CO₂ concentration gradients calculated from NICAM-TM CO₂ data near a CME measurement location. We collected eight NICAM-TM CO₂ data points from four model
20 grids adjacent to a CME measurement location at times before and after CME measurement, and linearly interpolated them to the CME measurement location and time. The red line in Figure 3(a) shows a CO₂ vertical profile determined in this manner. This CO₂ vertical profile was designated as “CME_obs.” profile. [Observations by satellite-borne nadir-viewing sensors like TANSO-FTS have much lower vertical resolution than aircraft observations. Therefore, we smoothed the CME_obs. profile to fit its vertical resolution to the vertical resolution of corresponding TIR CO₂ profile by](#)
25 [applying TIR CO₂ averaging kernel functions \(AK\) to the CME_obs. profile, as follows \(Rodgers and Connor, 2003\):](#)

$$\mathbf{x}_{\text{CME_AK}} = \mathbf{x}_{\text{a priori}} + \mathbf{A}(\mathbf{x}_{\text{CME_obs.}} - \mathbf{x}_{\text{a priori}}). \quad (1)$$

Here, $\mathbf{x}_{\text{CME_obs.}}$ and $\mathbf{x}_{\text{a priori}}$ are the CME_obs. and a priori CO₂ profiles, respectively. CME_obs. data with TIR CO₂ averaging kernels was designated as “CME_AK”, as indicated by the blue line in Figure 3(a).

We set two different criteria for the time difference between TANSO-FTS TIR and CME CO₂ profiles used for selection of
30 coincident pairs: a 24-h difference and a 72-h difference. Figure 4 shows a comparison of the results over Narita [a](#)Airport for coincident pairs with a 24- or 72-h time difference. Both averages and 1- σ standard deviations of differences between TIR

and CME CO₂ data selected using the 24- and 72-h thresholds were comparable, as shown in Figure 4, which means that the use of these two time difference criteria does not alter any conclusions drawn from comparisons of TIR and CME CO₂ data. The same was generally applied generally to comparisons over the other airports shown in Figure 1. Hence, we adopted a 72-h time difference between TIR and CME CO₂ measurement times for selecting coincident pairs to increase the number of pairs available.

We selected coincident pairs of TIR and CME_AK CO₂ profiles by applying the thresholds of a 300-km distance and a 72-h time difference and calculated the difference in CO₂ concentrations (TIR minus CME_AK) for each retrieval grid layer. All the airports we used were then divided into four latitude bands (40°S–20°S, 20°S–20°N, 20°N–40°N, and 40°N–60°N), and average differences were calculated for each latitude band, retrieval layer, and season (northern spring, MAMN; northern summer, JJA; northern fall, SON; and northern winter, DJF). The signs of the calculated average differences were flipped and defined as “bias-correction values” for the 28 retrieval grid layers, four latitude bands, and four seasons. The numbers of coincident pairs of TIR and CME_AK CO₂ profiles varied depending on latitude band and season. The largest number of coincident pairs was obtained in the latitude band of 20°N–40°N including Narita airport, where 506–2501 pairs were obtained. 63–310 and 77–472 coincident pairs were obtained at 40°S–20°S and 40°N–60°N, respectively. The comparison area for low latitudes was extended to a band of 20°S–20°N, because the number of coincident pairs in that region was smaller (0–341) than in other latitude bands; nevertheless, there were no coincident pairs at 20°S–20°N in the JJA seasons of 2011 and 2012. The number of coincident pairs was smallest (0–30) at 20°S–0° and at 20°S–0°; no data were collected there after September 2010. Thus, all bias-correction values for 20°S–20°N after the SON season of 2010 were determined based on data from 0°–20°N.

4.2 Comparison of TIR CO₂ data with NICAM-TM CO₂ data

In this study, we compared monthly averaged TANSO-FTS TIR and NICAM-TM CO₂ data. We used 2.5° grid data from NICAM-TM glevel-5 CO₂ simulations, and calculated monthly averaged TIR and NICAM-TM CO₂ data for each of these 2.5° grids. Here, we interpolated the NICAM-TM CO₂ data from 40 vertical levels into CO₂ concentrations at the 28 retrieval grid layers of TIR CO₂ data. Besides TIR CO₂ data, a priori CO₂ data and TIR CO₂ averaging kernel functions data were also averaged for each month and each 2.5° grid. For each of the 2.5° grids, we applied the monthly averaged TIR CO₂ averaging kernel functions to the corresponding monthly averaged NICAM-TM CO₂ profiles using expression (1) with the corresponding monthly averaged a priori CO₂ profiles. We then calculated differences in CO₂ concentrations between monthly averaged TIR data and monthly averaged NICAM-TM data with TIR averaging kernel functions for each grid. Here, two types of differences were calculated between TIR CO₂ data and NICAM-TM CO₂ data with TIR CO₂ averaging kernel functions: (1) the difference with respect to the original TIR CO₂ data and (2) the difference with respect to bias-corrected TIR CO₂ data to which the bias-correction values described above were applied.

TIR CO₂ averaging kernel functions depend on TIR measurement spectral noise, a priori CO₂ profile variability, and CO₂ Jacobians. Of these three parameters, covariance matrices of the TIR measurement noise and a priori CO₂ profile were set in

the same manner for all TIR V1 L2 CO₂ data (Saitoh et al., 2016). The CO₂ Jacobians depend on temperature and CO₂ profiles, and therefore change with location and time. However, TIR CO₂ averaging kernel functions showed nearly identical structures with each other when collected for each 2.5° grid in one month, which means that applying the monthly averaged TIR CO₂ averaging kernel functions did not affect the conclusions of this study.

5 Results

5.1 Bias of TIR LT and MT CO₂ concentrations

Figure 5 presents a comparison between TANSO-FTS TIR V1 and CME_AK CO₂ profiles over Narita Airport in each season in 2010. In all seasons, TIR CO₂ data in the LT and MT regions had negative biases against CME_AK CO₂ data. The largest negative biases in TIR CO₂ data were found in the MT region centered at 500–400 hPa. The peak of the negative biases in spring and summer occurred at ~400 hPa, slightly higher than the peak pressure level in fall and winter (~500 hPa), which corresponds to the pressure level at which the TIR CO₂ averaging kernels exhibited their highest sensitivity in each season. Saitoh et al. (2016) showed that TIR V1 CO₂ data agreed well with CME level flight CO₂ data in the UT region (287–196 hPa) corresponding to retrieval layers 9 and 10. As indicated by the solid black lines in Figure 5, the negative biases in the TIR CO₂ data against CME ascending and descending flight CO₂ data decreased as altitude increased, which is consistent with the results of Saitoh et al. (2016).

Figure 6 shows differences between TANSO-FTS TIR V1 and CME_AK CO₂ data in the LT and MT regions in retrieval layers 3–8 for each latitude band and each season. TIR CO₂ data had consistent negative biases of 1–1.5% against CME_AK CO₂ data in all retrieval layers from 736 to 287 hPa, with the largest negative biases at in retrieval layers 5–6 (541–398 hPa (retrieval layers 5–6)) for all latitude bands and seasons, except for 40°S–20°S in the DJF seasons of 2011 and 2012. Here, we have omitted a detailed discussion of TIR CO₂ data at pressure levels below 736 hPa (retrieval layers 1–2 (736 hPa)), because TIR measurements have relatively low sensitivity to CO₂ concentrations in these layers, as shown in Figure 3(b). The largest negative biases, up to 7.3 ppm, existed in low latitudes during the JJA season, as indicated by the red line in the upper panel of Figure 6(b), while there were no coincident pairs of TIR and CME CO₂ data in the same season of 2011 and 2012. As presented in Table 2, the negative biases in TIR CO₂ data were larger in spring (MAM) and summer (JJA) than in fall (SON) and winter (DJF) in northern middle latitudes (20°N–40°N), as was the case for UT comparisons presented in Saitoh et al. (2016). On a global scale, the seasonality of negative biases was not clear, given the relatively large 1-σ standard deviations (horizontal bars in the top panels of Figure 6), although these biases tended to be larger in the spring hemisphere than in the fall hemisphere within each latitude band. Comparing results among the three years, the negative biases in TIR CO₂ data slightly increased over time in some latitude bands and seasons, but not as sharply as in the UT CO₂ comparisons discussed in Saitoh et al. (2017). Note that the number of comparison pairs used in Figure 6 varied among latitude bands; the largest number occurred at 20°N–40°N, which includes Narita Airport, Japan, and the number of coincident profiles decreased in low latitudes and the Southern Hemisphere, where there are fewer airports.

5.2 Validity of bias correction based on CME data

Negative biases in TANSO-FTS TIR V1 CO₂ data in the LT and MT regions did not exhibit evident dependence on season or year, as shown in Figure 6. However, it is difficult to discern whether bias assessment using TIR CO₂ data over airports reflects the typical features of each latitude band due to the limited airport locations. Therefore, we validated the applicability of the bias-correction values based on comparisons with CME_AK CO₂ data over the entire area of each latitude band by comparing TIR CO₂ data to NICAM-TM CO₂ data to which TIR CO₂ averaging kernel functions were applied on a global scale. Figure 7 shows the frequency distributions of differences in monthly averaged CO₂ concentrations between TIR and NICAM-TM CO₂ data in all retrieval layers from 736 to 287 hPa in all 2.5° grids over the latitude range of 40°S to 60°N. As shown by the dashed lines in Figure 7, the mode values of the frequency distributions generally corresponded to the median values, indicating that TIR CO₂ data did not have locally distorted biases against NICAM-TM CO₂ data. In addition, negative biases of TIR CO₂ data against NICAM-TM CO₂ data in all seasons slightly increased by 1 ppm or less per year over time in all seasons, judging from the mode values presented in the top left boxes of Table 3, although the increase in negative biases was not much evident as in the comparisons over airports shown in Figure 6; this may be partly because of slightly high growth rate of NICAM-TM simulations (2.4 ppm/yr) compared to in-situ observations (2.2 ppm/yr).

The ~~solid~~thick lines in Figure 7 show frequency distributions of differences between NICAM-TM CO₂ data and bias-corrected TIR CO₂ data to which the bias-correction values defined for each retrieval layer, latitude band, and season were applied. The mode values presented in the top right boxes of Table 3, which were nearly identical to the median values, were closer to zero in all three years. In addition, variability in the differences, as indicated by the width of the distribution, between bias-corrected TIR and NICAM-TM CO₂ data was comparable to or smaller than that between the original TIR and NICAM-TM CO₂ data; this can be seen by comparisons in values of frequencies at the mode values between before and after applying the bias-corrections values, presented in Table 3. This demonstrates the validity of the 288 bias-correction values defined for six retrieval layers (~~3–8~~from 736 to 287 hPa), four latitude bands (0°S–20°S, 20°S–20°N, 20°N–40°N, and 40°N–60°N), and four seasons of 2010–2012. We thus conclude that the bias-correction values defined based on comparisons in limited areas near airports are generally applicable to TIR CO₂ data in areas other than the airport locations. However, there were some exceptions during the JJA season. As indicated by the ~~solid~~thick black line in Figure 7(c), the frequency distribution of differences between bias-corrected TIR and NICAM-TM CO₂ data in the JJA season of 2010 had a clear bimodal feature, with one of the mode values located near 4 ppm.

We divided the frequency distribution in the JJA season of 2010 into three categories based on the retrieval layers: 736–541 hPa (retrieval layers 3–4), 541–398 hPa (retrieval layers 5–6), and 398–287 hPa (retrieval layers 7–8), as shown in Figure 8. A frequency distribution with a mode of 4 ppm was obtained from bias-corrected TIR CO₂ data in the MT region above 541 hPa (retrieval layer 5), especially on in retrieval layers 398–287 hPa. That is, TIR CO₂ data on 398–287 hPa in retrieval layers 7–8 in the JJA season of 2010 were clearly overcorrected when applying the bias-correction values defined in this

study. [In the retrieval layers of 736–541 hPa](#)~~In retrieval layers 3–4~~, the mode value of the frequency distribution after bias-correction was close to zero and the width of the distribution narrowed, demonstrating the validity of the corresponding bias-correction value. For the JJA seasons of 2011 and 2012, bias-correction values could not be determined because there were no coincident pairs between TIR and CME CO₂ data over airports; therefore, we substituted the bias-correction value for the same season of 2010. The frequency distribution of the differences between NICAM-TM and TIR CO₂ data after bias-correction in the JJA season of 2011 had a somewhat bimodal shape, while that in the JJA season of 2012 did not have any bimodal structure, as shown in Figure 7(c). The negative bias of the original TIR CO₂ data against NICAM-TM CO₂ data in the JJA season of 2012 was larger than that in the JJA season of 2010; thus, applying the bias-correction value for 2010 to the 2012 TIR CO₂ data did not lead to any evident overcorrection.

Next, we divided the frequency distribution in [the retrieval layers of 3987–287 hPa](#)~~8~~ in the JJA season of 2010, shown in Figure 8, into four latitude bands. Judging from the results presented in Figure 9, overcorrection of the negative biases in TIR CO₂ data against NICAM-TM CO₂ data occurred at 20°S–20°N and 40°N–60°N; TIR CO₂ data were markedly overcorrected by the bias-correction value based on comparisons of CME CO₂ data over airports, especially in the latitude band of 20°S–20°N. As shown in the upper panel of Figure 6, negative biases in TIR CO₂ data against CME CO₂ data over airports in low latitudes during the JJA season were clearly larger than the biases found in other latitudes and seasons. Judging from comparisons of global NICAM-TM CO₂ data, however, applying bias-correction values based on the negative biases observed over airports to TIR CO₂ data over the entire area of 20°S–20°N led to overcorrections in most cases.

6. Discussion

Any uncertainties in a priori data can affect retrieval results. A priori CO₂ data taken from the NIES-TM05 model (Saeki et al., 2013b) was used in the TANSO-FTS TIR V1 CO₂ retrieval processing, and exhibited consistent negative biases against CME CO₂ data in [the troposphere and the lower stratosphere](#)~~retrieval layers 3–8~~. As discussed in Saitoh et al. (2016), the negative biases in a priori CO₂ data were one likely reason for negative biases in retrieved CO₂ concentrations in the UTLS region. The same pattern holds for negative biases in TIR CO₂ data in the LT and ~~MTL~~ regions. However, negative biases in retrieved TIR CO₂ data were larger than those of a priori CO₂ data in the LT and MT regions, as shown in Figure 5. Furthermore, the vertical and latitudinal structures of the negative biases in TIR CO₂ data did not always correspond to those in a priori CO₂ data. Although negative biases in a priori CO₂ data surely contribute to negative biases in TIR V1 CO₂ data in the LT and MT regions, there are likely other considerable sources of [TIR CO₂](#) negative biases.

Uncertainty in atmospheric temperature data could affect CO₂ retrievals. As shown in Figure 7(a) of Saitoh et al. (2009), uncertainties in retrieved CO₂ concentrations due to uncertainties in atmospheric temperature were largest in the UT, upper MT, and LT regions; a bias of 1 K in atmospheric temperature can yield up to ~10% uncertainty in retrieved CO₂ concentrations in the MT and LT regions. However, simultaneous retrieval of atmospheric temperature in the V1 CO₂ retrieval algorithm could decrease the effect on CO₂ retrieval results. In addition to that, no evidence has been reported that

the JMA-GPV temperature data used as initial values (equal to a priori values) in the TIR V1 CO₂ retrieval processing have biases over such wide latitudinal areas, as in this study. Thus, uncertainty in atmospheric temperature is not a primary cause of negative biases in TIR CO₂ data in the LT and MT regions. Although the effect of uncertainty in H₂O data on CO₂ retrieval results could be also decreased by simultaneous retrieval of H₂O with CO₂ in the TIR V1 algorithm, water vapor is abundant in the tropics, so that we cannot deny the possibility of its effect on CO₂ retrieval results. Similarly, error in the judgement of cloud contamination in low latitudes with high cloud occurrence frequency may affect CO₂ retrieval results.

As shown in Figure 6, the largest negative biases in TIR V1 CO₂ data existed in the MT region in low latitudes (20°S–20°N) during the JJA season. Degrees of freedom (DF) of TIR V1 CO₂ data were highest in low latitudes, exceeding 2.2 in all seasons, which means retrieved CO₂ concentrations there contained more information coming from TANSO-FTS TIR L1B spectra and thus were relatively less constrained to a priori concentrations.

Kataoka et al. (2014) reported biases in TANSO-FTS TIR V130.131 L1B radiance spectra, which were a previous version of the V161 L1B data used in TIR V1 L2 CO₂ retrieval, on the basis of a double difference method. Similar analysis for the V161 L1B spectra is in progress. Kuze et al. (2016) summarized updates in the processing method for TANSO-FTS L1B spectra and. They showed that the V161 and newer version (V201) of TANSO-FTS L1B spectra still had ve considerable uncertainties via theoretical simulations. As shown in Figure 6, the largest negative biases in TIR V1 CO₂ data existed in the MT region in middle and low latitudes during spring and summer, where TANSO-FTS TIR measurements have relatively large sensitivity to CO₂ concentrations and thus the retrievals are less constrained to a priori concentrations. Kataoka et al. (2014) and Kuze et al. (2016) demonstrated that TANSO-FTS TIR L1B spectra had considerable radiance biases, which were largest at around 15- μ m CO₂ absorption band.

~~This implies that biases in L1B spectra are a major cause of the negative biases in retrieved CO₂ concentrations, as Saitoh et al. (2016) noted in the UT region.~~ In the TIR V1 CO₂ retrieval algorithm, we simultaneously retrieved surface temperature and surface emissivity with CO₂ concentration as a correction parameter for radiance biases in the V161 spectra, as explained in Saitoh et al. (2016). In the CO₂ retrieval, these surface parameters were retrieved to correct the radiance spectral biases separately in the three spectral regions of the 15- μ m (690–715 cm⁻¹, 715–750 cm⁻¹, and 790–795 cm⁻¹), 10- μ m (930–990 cm⁻¹), and 9- μ m bands (1040–1090 cm⁻¹). As reported in Saitoh et al. (2016), the simultaneous retrieval of surface parameters for correction of radiance spectral biases increased the number of normally retrieved CO₂ data (by roughly 1.5 times over Narita aAirport). This demonstrates a certain level of validity for the correction of radiance spectral biases through simultaneous retrieval of surface parameters for the V161 spectra. However, we note that retrieving surface parameters for radiance spectral bias correction at each wavelength band may affect retrieved CO₂ concentrations, and remaining radiance spectral biases after correction at each wavelength band may also affect retrieved CO₂ concentrations.

To examine the effect of the simultaneous retrieval of surface parameters at each of the three wavelength bands on retrieved CO₂ concentrations, The V1 CO₂ retrieval algorithm utilized 15 μ m, 10 μ m, and 9 μ m bands. Here, we performed test retrievals of CO₂ concentrations using V161 spectra in four cases: using all three of these bands, in the same manner as the V1 algorithm; using two bands, 15- μ m and 10- μ m; using two bands, 15- μ m and 9- μ m; and using the 15- μ m band only.

Figure 10 shows the CO₂ retrieval results for ~~two~~three TANSO-FTS observations ~~over Narita airport in April 2010 in low latitudes during summer and in northern middle latitudes in spring, where most TIR V1 CO₂ data had negative biases.~~ As ~~shown indicated by the black lines~~ in Figure 10(a), negative biases in TIR CO₂ concentrations against nearby CME CO₂ concentrations in the LT and MT regions became notably smaller when using the 15- μ m and 9- μ m bands (black dashed lines) and the 15- μ m band only (black dashed-dotted lines), both conditions that did not use the 10- μ m band. It is clear that using the 9- μ m band did not contribute to negative biases in retrieved CO₂ concentrations, judging from the minor difference in CO₂ concentrations between the use of all three bands (~~solid thick~~ lines) and the use of the 15- μ m and 10- μ m bands (dotted lines). In addition, there were no major differences in retrieved CO₂ concentrations among the four retrieval cases when the original V1 CO₂ profile did not have distinct negative biases, as ~~shown illustrated by the gray lines~~ in Figure 10(b). According to theoretical calculations shown in Figure 13 in Kuze et al. (2016), there were no distinct radiance biases in the 10- μ m band in the latest version of the TANSO-FTS TIR spectra. If it is true for observed TIR radiances, our test retrievals imply that simultaneous retrieval of surface parameters for TIR spectra at the 10- μ m band with less radiance bias worsened CO₂ retrieval results. From these test retrieval results demonstrate that, we conclude that using the 10- μ m band in conjunction with the 15- μ m and 9- μ m bands in the V1 retrieval algorithm is a probable cause of the negative biases in retrieved CO₂ concentrations in the LT and MT regions, although this cannot fully explain the biases.

CO₂ absorption at 15 μ m is considerably larger than that at 9 or 10 μ m. However, measurements in the 9- μ m and 10- μ m bands are most sensitive to CO₂ concentrations in the LT and MT regions; the peak sensitivity of the 9- μ m and 10- μ m bands occurred on retrieval layers 7363–541 hPa₄ and 5415–398 hPa₆, respectively, judging from CO₂ Jacobian values. Therefore, using the 9- μ m and 10- μ m bands in conjunction with the 15- μ m band should be useful for retrieving CO₂ vertical profiles. In fact, in the case of ~~the retrieval result low latitudes in summer~~ shown in Figure 10(a), the degree of freedom of CO₂ retrieval was 12.9308 when using the 15- μ m band only, and it increased to 12.9409, 1.95244, and 1.96242 when adding the 9- μ m band, the 10- μ m band, and both the 9- μ m and 10- μ m bands, respectively. ~~According to Figure 13 in Kuze et al. (2016), there was no distinct uncertainty in the 10 μ m band in the latest version of the TANSO-FTS TIR spectra. Our test retrievals imply that simultaneous retrieval of surface parameters for the 10 μ m band over or under corrected the spectral bias of V161 spectra.~~ In the next update of the CO₂ retrieval algorithm for TANSO-FTS TIR spectra, we should consider an improved method for correcting radiance spectral biases in CO₂ retrieval processing or adopting the correction of TIR L1B spectra themselves proposed by Kuze et al. (2016).

Bias-correction values determined based on comparisons of CME CO₂ data over airports overcorrected negative biases in TIR CO₂ data in the upper MT region from 398 to 287 hPa (layers 7–8) in low latitudes (20°S–20°N) during the JJA season, as shown in Figure 9. The CME data that determined the bias-correction values of the 20°S–20°N latitude band were concentrated in Southeast Asia, as illustrated in Figure 1: BKK (Bangkok), SIN (Singapore), and CGK (Jakarta). In addition, the bias-correction values for the 20°S–20°N latitude band after the SON season of 2010 were determined from comparisons of CME data at 0°–20°N, because no data were collected at 20°S–0° after September 2010, as mentioned above. Figure 11 shows differences between TIR CO₂ data with no bias correction and NICAM-TM CO₂ data with TIR CO₂

averaging kernel functions ~~on 682 hPa in retrieval layers 3 and 314 hPa~~ in July 2010. ~~As shown in the lower panel of Figure 11, in most areas of retrieval layer 8 at 0°–20°N, TIR CO₂ data on 314 hPa had negative biases against NICAM-TM CO₂ data in most areas at 0°–20°N,~~ and the negative biases were largest near airport locations in ~~SouthEast~~ East Asia. At 20°S–0°, on the other hand, TIR CO₂ data ~~in retrieval layer 8 on 314 hPa~~ were closer to NICAM-TM CO₂ data than at 0°–20°N.

5 Relying on NICAM-TM CO₂ data, which incorporates CONTRAIL CO₂ data in the inversion, application of bias-correction values determined mainly from comparisons of CME CO₂ data in the MT region at 0°–20°N to TIR CO₂ data over the entire area of low latitudes including 20°S–0° produced widespread overcorrection.

In general, there are few areas where we can obtain reliable in situ CO₂ data for validation analysis. In particular, there are very few in situ CO₂ data in the free troposphere where TIR observations are most sensitive, compared to the surface. In low

10 latitudes, there are relatively strong updrafts, and thus there are larger uncertainties among models than in other areas due to differences in the parameterization of vertical transport. ~~Therefore, a priori CO₂ concentrations taken from the NIES-TM05 model (Saeki et al., 2013b) probably have larger uncertainties in the MT region in low latitudes. As retrieved TIR CO₂ concentrations were to some extent constrained by a priori concentrations, they possibly had more~~

15 ~~In retrieval from TIR spectra, the more atmospheric layers in which we retrieve CO₂ concentrations, the lower the information content of the retrieval result in each layer becomes; as a result, the retrieved concentrations are constrained by a priori model data. Thus, there is a high possibility of large biases attributed to the a priori uncertainties in the MT region~~ retrieved TIR CO₂ concentrations in low latitudes. More in-situ CO₂ data in the upper atmosphere in low latitudes are needed to validate both satellite data and model results. ~~Although HIAPER Pole-to-Pole Observations (HIPPO) data (Wofsy et al., 2011) are not suitable for a comprehensive validation study as in this study due to their limited observation periods, HIPPO CO₂ data are useful to validate CO₂ vertical profiles observed by satellite-borne sensors and simulated in models (Kulawik et al., 2013).~~

20 In addition, there may also be large biases in retrieved CO₂ data in local source and sink regions, where model data are more variable depending on the surface flux dataset. In such areas, it is difficult to determine bias-correction values that can be applicable over a vast area; it is true in the case of 40°N–60°N. In conclusion, comprehensive validation analysis of satellite data is still needed to evaluate accuracy both in background regions and in regions with high CO₂ variability.

25 Reconsideration of the setting of retrieval ~~grid layers~~ grid is also needed so that measurement information should be included more prominently in TIR CO₂ retrieval results.

Overall, the bias-correction values evaluated in each retrieval layer, latitude band, and season (Figure 6) can be applied to corresponding TIR CO₂ data, except at 20°S–20°N during the JJA seasons of 2011 and 2012~~4~~, when bias-correction values were not determined due to a lack of coincident CME CO₂ data. In these two cases, we recommended applying bias-correction value 0.5 ppm and 1.0 ppm larger than the corresponding bias-correction value for 2010 to TIR CO₂ data for 2011 and 2012, respectively, judging from comparison results between the original TIR and NICAM-TM CO₂ data.

7. Summary

We evaluated biases of the GOSAT/TANSO-FTS TIR V1 L2 CO₂ product in the LT and MT regions (736–287 hPa) by comparing the TIR CO₂ profiles with coincident CONTRAIL CME CO₂ profiles over airports from 2010 to 2012. Coincident criteria for comparisons of a 300-km distance and a 72-h time difference yielded a sufficient number of coincident pairs, except in low latitudes (20°S–20°N) during JJA seasons of 2011 and 2012. Comparisons between TIR CO₂ profiles and CME CO₂ profiles to which TIR CO₂ averaging kernel functions ~~were had been~~ applied showed that the TIR V1 CO₂ data had consistent negative biases of 1–1.5% against CME CO₂ data in the LT and MT regions; the negative biases were the largest on 541–398 hPa (~~in retrieval layers 5–6 (541–398 hPa)~~), and were larger in spring and summer than in fall and winter in northern middle latitudes, as is the case in the UT region (287–196 hPa). Our test retrieval simulations showed that using the 10- μ m CO₂ absorption band (930–990 cm⁻¹), in addition to the 15- μ m (690–750 cm⁻¹ and 790–795 cm⁻¹) and 9- μ m (1040–1090 cm⁻¹) bands, ~~increased probably caused these~~ negative biases in retrieved CO₂ concentrations in the LT and MT regions, suggesting that simultaneous retrieval of surface parameters for radiance bias correction at the 10- μ m band ~~worsenever or under corrected~~ CO₂ retrieval results, the spectral biases inherent to TANSO-FTS V161-L1B spectra.

We then performed global comparisons between TIR V1 CO₂ data and NICAM-TM CO₂ data with considering TIR CO₂ averaging kernel functions to confirm the validity of the bias assessment over airports. Differences in CO₂ concentrations between TIR and NICAM-TM data approached an average of zero after application of the bias-correction values to TIR CO₂ data, demonstrating that the bias-correction values evaluated over airports in limited areas are applicable to TIR CO₂ data for the entire areas of 40°S–60°N. Note that applying the bias correction value at 20°S–20°N in the upper MT region (398–287 hPa) during the JJA season resulted in overcorrection of TIR CO₂ data.

This study presented bias-correction values for the GOSAT/TANSO-FTS TIR V1 L2 CO₂ product evaluated in the LT and MT region (~~for retrieval layers 7363–287 hPa~~)⁸ in each latitude band and each season of 2010–2012. This information should be useful for further analyses, including CO₂ surface flux estimation and transport process studies using TIR CO₂ data in the free troposphere, and also helpful for evaluating wavelength-dependent ~~radiance spectral~~ biases in TANSO-FTS TIR spectra to improve TIR CO₂ retrieval algorithm ~~for the TIR spectra~~.

25 Data availability

GOSAT/TANSO-FTS TIR V1 L2 and a priori NIES-TM05 CO₂ data and TIR CO₂ averaging kernel data are available at <http://www.gosat.nies.go.jp/en/>. Contact the CONTRAIL project (<http://www.cger.nies.go.jp/contrail/index.html>) to access CONTRAIL CME CO₂ data. Contact Y. Niwa for detailed information on NICAM-TM CO₂ simulations. Contact the corresponding author, N. Saitoh, to obtain the table of bias-correction values for TIR V1 L2 CO₂ data evaluated in this study.

Acknowledgment.

We thank all the members of the GOSAT Science Team and their associates. We are also grateful to the engineers of Japan Airlines, the JAL Foundation, and JAMCO Tokyo for supporting the CONTRAIL project. This study was funded by the Japan Aerospace Exploration Agency (JAXA). This study was performed within the framework of the GOSAT Research
5 Announcement.

References

- [Andres, R. J., Boden, T., and Marland, G.: Monthly Fossil-Fuel CO₂ Emissions: Mass of Emissions Gridded by One Degree Latitude by One Degree Longitude, Carbon Dioxide Information Analysis Center, Oak Ridge National Laboratory, U.S. Department of Energy, Oak Ridge, Tenn., USA, doi:10.3334/CDIAC/ffe.MonthlyMass.2013, 2013.](https://doi.org/10.3334/CDIAC/ffe.MonthlyMass.2013)
- 10 Barkley, M. P., Frieß, U., and Monks, P. S.: Measuring atmospheric CO₂ from space using Full Spectral Initiation (FSI) WFM-DOAS, *Atmos. Chem. Phys.*, 6, 3517-3534, 2006.
- Barnes, E. A., Parazoo, N., Orbe, C., and Denning, A. S.: Isentropic transport and the seasonal cycle amplitude of CO₂, *J. Geophys. Res. Atmos.*, 121, doi:10.1002/2016JD025109, 2016.
- Basu, S., Guerlet, S., Butz, A., Houweling, S., Hasekamp, O., Aben, I., Krummel, P., Steele, P., Langenfelds, R., Torn, M.,
15 Biraud, S., Stephens, B., Andrews, A., and Worthy, D.: Global CO₂ fluxes estimated from GOSAT retrievals of total column CO₂, *Atmos. Chem. Phys.*, 13, 8695-8717, 2013.
- Basu, S., Krol, M., Butz, A., Clerbaux, C., Sawa, Y., Machida, T., Matsueda, H., Frankenberg, C., Hasekamp, O. P., and Aben, I.: The seasonal variation of the CO₂ flux over Tropical Asia estimated from GOSAT, CONTRAIL, and IASI, *Geophys. Res. Lett.*, 41, 1809-1815, 2014.
- 20 Brenninkmeijer, C. A. M. et al.: Civil Aircraft for the regular investigation of the atmosphere based on an instrumented container: The new CARIBIC system, *Atmos. Chem. Phys.*, 7, 4953-4976, 2007.
- Buchwitz, M., de Beek, R., Burrows, J. P., Bovensmann, H., Warneke, T., Notholt, J., Meirink, J. F., Goede, A. P. H., Bergamaschi, P., Körner, S., Heimann, M., and Schulz, A.: Atmospheric methane and carbon dioxide from SCIAMACHY satellite data: initial comparison with chemistry and transport models, *Atmos. Chem. Phys.*, 5, 941-962, 2005.
- 25 Butz, A. et al.: Toward accurate CO₂ and CH₄ observations from GOSAT, *Geophys. Res. Lett.*, 38, doi:10.1029/2011GL047888, 2011.
- Chahine, M., Barnett, C., Olsen, E. T., Chen, L., and Maddy, E.: On the determination of atmospheric minor gases by the method of vanishing partial derivatives with application to CO₂, *Geophys. Res. Lett.*, 32, doi:10.1029/2005GL024165, 2005.
- Chédin, A., Serrar, S., Armante, R., Scott, N. A., and Hollingsworth, A.: Signatures of annual and seasonal variations of CO₂
30 and other greenhouse gases from comparisons between NOAA TOVS observations and radiation model simulations, *J. Climate*, 15, 95-116, 2002.

- Chédin, A., Serrar, S., Scott, N. A., Crevoisier, C., and Armante, R.: First global measurement of midtropospheric CO₂ from NOAA polar satellites, *J. Geophys. Res.*, 108, doi:10.1029/2003JD003439, 2003.
- Chédin, A., Serrar, S., Scott, N. A., Pierangelo, C., and Ciais, P.: Impact of tropical biomass burning emissions on the diurnal cycle of upper tropospheric CO₂ retrieved from NOAA 10 satellite observations, *J. Geophys. Res.*, 110, doi:10.1029/2004JD005540, 2005.
- Chevallier, F., Fisher, M., Peylin, P., Serrar, S., Bousquet, P., Bréon, F.-M., Chédin, A., and Ciais, P.: Inferring CO₂ sources and sinks from satellite observations: Method and application to TOVS data, *J. Geophys. Res.*, 110, doi:10.1029/2005JD006390, 2005.
- Chevallier, F., Palmer, P. I., Feng, L., Boesch, H., O'Dell, C. W., and Bousquet, P.: Toward robust and consistent regional CO₂ flux estimates from in situ and spaceborne measurements of atmospheric CO₂, *Geophys. Res. Lett.*, 41, 1065-1070, 2014.
- Cogan, A. J., Boesch, H., Parker, R. J., Feng, L., Palmer, P. I., Blavier, J.-F. L., Deutscher, N. M., Macatangay, R., Notholt, J., Roehl, C., Warneke, T., and Wunch, D.: Atmospheric carbon dioxide retrieved from the Greenhouse gases Observing SATellite (GOSAT): Comparison with ground-based TCCON observations and GEOS-Chem model calculations, *J. Geophys. Res.*, 117, doi:10.1029/2012JD018087, 2012.
- Connor, B., Bösch, H., McDuffie, J., Taylor, T., Fu, D., Frankenberg, C., O'Dell, C., Payne, V. H., Gunson, M., Pollock, R., Hobbs, J., Oyafuso, F., and Jiang, Y.: Quantification of uncertainties in OCO-2 measurements of XCO₂: simulations and linear error analysis, *Atmos. Meas. Tech.*, 9, 5227–5238, 2016.
- Crevoisier, C., Heilliette, S., Chédin, A., Serrar, S., Armante, R., and Scott, N. A.: Midtropospheric CO₂ concentration retrieval from AIRS observations in the tropics, *Geophys. Res. Lett.*, 31, doi:10.1029/2004GL020141, 2004.
- Crevoisier, C., Chédin, A., Matsueda, H., Machida, T., Armante, R., and Scott, N. A.: First year of upper tropospheric integrated content of CO₂ from IASI hyperspectral infrared observations *Atmos. Chem. Phys.*, 9, 4797-4810, 2009.
- Crisp, D., Pollock, H. R., Rosenberg, R., Chapsky, L., Lee, R. A. M., Oyafuso, F. A., Frankenberg, C., O'Dell, C. W., Bruegge, C. J., Doran, G. B., Eldering, A., Fisher, B. M., Fu, D., Gunson, M. R., Mandrake, L., Osterman, G. B., Schwandner, F. M., Sun, K., Taylor, T. E., Wennberg, P. O., and Wunch, D.: The on-orbit performance of the Orbiting Carbon Observatory-2 (OCO-2) instrument and its radiometrically calibrated products, *Atmos. Meas. Tech.*, 10, 59–81, 2017.
- Intergovernmental Panel on Climate Change (IPCC): Contribution of Working Group I to the Fifth Assessment Report of the Intergovernmental Panel on Climate Change, Cambridge University Press, Cambridge, United Kingdom and New York, NY, USA, 2013.
- Gurney, K. R. et al.: Towards robust regional estimates of CO₂ sources and sinks using atmospheric transport models, *Nature*, 415, 626-630, 2002.
- Gurney, K. R. et al.: Transcom 3 inversion intercomparison: Model mean results for the estimation of seasonal carbon sources and sinks, *Geosci. Model Dev.*, doi:10.1029/2003GB002111, 2004.

- Kataoka, F., Knuteson, R. O., Kuze, A., Suto, H., Shiomi, K., Harada, M., Garms, E. M., Roman, J. A., Tobin, D. C., Taylor, J. K., Revercomb, H. E., Sekio, N., Higuchi, R., and Mitomi, Y.: TIR spectral radiance calibration of the GOSAT satellite borne TANSO-FTS with the aircraft-based S-HIS and the ground-based S-AERI at the Railroad Valley desert playa, *IEEE T. Geosci. Remote*, 52, 89-105, 2014.
- 5 Kulawik, S. S., Jones, D. B. A., Nassar, R., Irion, F. W., Worden, J. R., Bowman, K. W., Machida, T., Matsueda, H., Sawa, Y., Biraud, S. C., Fischer, M. L., and Jacobson, A. R.: Characterization of Tropospheric Emission Spectrometer (TES) CO₂ for carbon cycle science, *Atmos. Chem. Phys.*, 10, 5601-5623, 2010.
- Kulawik, S. S. et al.: Comparison of improved Aura Tropospheric Emission Spectrometer CO₂ with HIPPO and SGP aircraft profile measurements, *Atmos. Chem. Phys.*, 13, 3205-3225, 2013.
- 10 Kuze, A., Suto, H., Nakajima, M., and Hamazaki, T.: Thermal and near infrared sensor for carbon observation Fourier-transform spectrometer on the Greenhouse Gases Observing Satellite for greenhouse gases monitoring, *Appl. Optics*, 48, 6716-6733, 2009.
- Kuze, A., Suto, H., Shiomi, K., Kawakami, S., Tanaka, M., Ueda, Y., Deguchi, A., Yoshida, J., Yamamoto, Y., Kataoka, F., Taylor, E. T. and Buijs, H.: Update on GOSAT TANSO-FTS performance, operations, and data products after more than 6
- 15 years in space, *Atmos. Meas. Tech.*, 9, 2445-2461, 2016.
- Machida, T., Matsueda, H., Sawa, Y., Nakagawa, Y., Hirofumi, K., Kondo, N., Goto, K., Nakazawa, T., Ishikawa, K., and Ogawa, T.: Worldwide measurements of atmospheric CO₂ and other trace gas species using commercial airlines, *J. Atmos. Ocean Tech.*, 25, 1744-1754, 2008.
- Machida, T., Tohjima, Y., Katsumata, K., and Mukai, H.: A new CO₂ calibration scale based on gravimetric one-step
- 20 dilution cylinders in National Institute for Environmental Studies - NIES 09 CO₂ Scale, 15th WMO/IAEA Meeting of Experts on Carbon Dioxide, Other Greenhouse Gases and Related Tracers Measurement Techniques, GAW Rep., 194, 165-169, World Meteorological Organization, Geneva, Switzerland, 2011.
- Maddy, E. S., Barnett, C. D., Goldberg, M., Sweeney, C., and Liu, X.: CO₂ retrievals from the Atmospheric Infrared Sounder: Methodology and validation, *J. Geophys. Res.*, 113, doi:10.1029/2007JD009402, 2008.
- 25 Maksyutov, S., Takagi, H., Valsala, V. K., Saito, M., Oda, T., Saeki, T., Belikov, D. A., Saito, R., Ito, A., Yoshida, Y., Morino, I., Uchino, O., Andres, R. J., and Yokota, T.: Regional CO₂ flux estimates for 2009-2010 based on GOSAT and ground-based CO₂ observations, *Atmos. Chem. Phys.*, 13, 9351-9373, 2013.
- Miyazaki, K., Patra, P. K., Takigawa, M., Iwasaki, T., and Nakazawa, T.: Global-scale transport of carbon dioxide in the troposphere, *J. Geophys. Res.*, 113, doi:10.1029/2007JD009557, 2008.
- 30 Niwa, Y., Patra, P. K., Sawa, Y., Machida, T., Matsueda, H., Belikov, D., Maki, T., Ikegami, M., Imasu, R., Maksyutov, S., Oda, T., Satoh, M. and Takigawa, M.: Three-dimensional variations of atmospheric CO₂: aircraft measurements and multi-transport model simulations, *Atmos. Chem. Phys.*, 11, 13359-13375, 2011a.
- Niwa, Y., Tomita, H., Satoh, M., and Imasu, R.: A three-dimensional icosahedral grid advection scheme preserving monotonicity and consistency with continuity for atmospheric tracer transport, *J. Meteor. Soc. Jpn.*, 89, 255-268, 2011b.

- Niwa, Y., Machida, T., Sawa, Y., Matsueda, H., Schuck, T. J., Brenninkmeijer, C. A. M., Imasu, R., and Satoh, M.: Imposing strong constraints on tropical terrestrial CO₂ fluxes using passenger aircraft based measurements, *J. Geophys. Res.*, 117, doi:10.1029/2012JD017474, 2012.
- Niwa, Y., Tomita, H., Satoh, M., Imasu, R., Sawa, Y., Tsuboi, K., Matsueda, H., Machida, T., Sasakawa, M., Belan, B., and Saigusa, N.: A 4D-Var inversion system based on the icosahedral grid model (NICAM-TM 4D-Var v1.0) – Part 1: Offline forward and adjoint transport models, *Geosci. Model Dev.*, 10, 1157–1174, doi:10.5194/gmd-10-1157-2017, 2017.
- O'Dell, C. W. et al.: The ACOS CO₂ retrieval algorithm - Part 1: Description and validation against synthetic observations *Atmos. Meas. Tech.*, 5, 99-121, 2012.
- Ota, Y. and Imasu, R.: CO₂ retrieval using thermal infrared radiation observation by Interferometric Monitor for Greenhouse Gases (IMG) onboard Advanced Earth Observing Satellite (ADEOS), *J. Meteorol. Soc. Jpn.*, 94, 471-490, 2016.
- Patra, P. K. et al.: Sensitivity of inverse estimation of annual mean CO₂ sources and sinks to ocean-only sites versus all-sites observational networks, *Geophys. Res. Lett.*, doi:10.1029/2005GL025403, 2006.
- Peters, W., Jacobson, A. R., Sweeney, C., Andrews, A. E., Conway, T. J., Masarie, K., Miller, J. B., Bruhwiler, L. M. P., Petron, G., Hirsch, A. I., Worthy, D. E. J., van der Werf, G. R., Randerson, J. T., Wennberg, P. O., Krol, M. C., and Tans, P. P.: An atmospheric perspective on North American carbon dioxide exchange: CarbonTracker", *PNAS*, 48, 104, 18925-18930, with updates documented at <http://carbontracker.noaa.gov>.
- Rodgers, C. D. and Connor, B. J.: Intercomparison of remote sounding instruments, *J. Geophys. Res.*, 108, 10.1029/2002JD002299, 2003.
- Saeki, T., Maksyutov, S., Saito, M., Valsala, V., Oda, T., Andres, R. J., Belikov, D., Tans, P., Dlugokencky, E., Yoshida, Y., Morino, I., Uchino, O., and Yokota, T.: Inverse Modeling of CO₂ Fluxes Using GOSAT Data and Multi-Year Ground-Based Observations, *SOLA*, 9, 45-50, 2013a.
- Saeki, T., Saito, R., Belikov, D., and Maksyutov, S.: Global high-resolution simulations of CO₂ and CH₄ using a NIES transport model to produce a priori concentrations for use in satellite data retrievals, *Geosci. Model Dev.*, 6, 81-100, 2013b.
- Saitoh, N., Imasu, R., Ota, Y., and Niwa, Y.: CO₂ retrieval algorithm for the thermal infrared spectra of the Greenhouse Gases Observing Satellite: potential of retrieving CO₂ vertical profile from high-resolution FTS sensor, *J. Geophys. Res.*, 114, doi:10.1029/2007JD011500, 2009.
- Saitoh, N., Kimoto, S., Sugimura, R., Imasu, R., Kawakami, S., Shiomi, K., Kuze, A., Machida, T., Sawa, Y. and Matsueda, H.: Algorithm update of GOSAT/TANSO-FTS TIR CO₂ product (Version 1) and validation of the UTLS CO₂ data using CONTRAIL measurements, *Atmos. Meas. Tech.*, 9, 2119–2134, 2016.
- Saitoh, N., Kimoto, S., Sugimura, R., Yamada, A., Imasu, S., Shiomi, K., Kuze, A., Machida, T., Sawa, Y. and Matsueda, H.: Time-series [and seasonal variations](#) of upper tropospheric CO₂ concentrations obtained with the GOSAT/TANSO-FTS [TIRthermal infrared](#) band, [in preparationsubmitted to SOLA, 2017](#).
- Satoh, M., Matsuno, T., Tomita, H., Miura, H., Nasuno, T. and Iga, S.: Nonhydrostatic icosahedral atmospheric model (NICAM) for global cloud resolving simulations, *J. Comput. Phys.*, 227, 3486–3514, 2008.

- Satoh, M., Tomita, H., Yashiro, H., Miura, H., Kodama, C., Seiki, T., Noda, A. T., Yamada, Y., Goto, D., Sawada, M., Miyoshi, T., Niwa, Y., Hara, M., Ohno, T., Iga, S., Arakawa, T., Inoue, T., and Kubokawa, H.: The Non-hydrostatic Icosahedral Atmospheric Model: description and development, *Progress in Earth and Planetary Science*, 1, 1–32, doi:10.1186/s40645-014-0018-1, 2014.
- 5 Strow, L. L. and Hannon, S. E.: A 4-year zonal climatology of lower tropospheric CO₂ derived from ocean-only Atmospheric Infrared Sounder observations, *J. Geophys. Res.*, 113, doi:10.1029/2007JD009713, 2008.
- Takagi, H. et al.: Influence of differences in current GOSAT XCO₂ retrievals on surface flux estimation, *Geophys. Res. Lett.*, 41, 2598-2605, 2014.
- Tomita, H. and Satoh, M.: A new dynamical framework of non- hydrostatic global model using the icosahedral grid, *Fluid Dyn. Res.*, 34, 357–400, doi:10.1016/j.fluiddyn.2004.03.003, 2004.
- 10 [van der Werf, G. R., Randerson, J. T., Giglio, L., Collatz, G. J., Mu, M., Kasibhatla, P. S., Morton, D. C., DeFries, R. S., Jin, Y., and van Leeuwen, T. T.: Global fire emissions and the contribution of deforestation, savanna, forest, agricultural, and peat fires \(1997– 2009\), *Atmos. Chem. Phys.*, 10, 11707–11735, doi:10.5194/acp-10-11707-2010, 2010.](#)
- 15 [Wada, A., Matsueda, H., Sawa, Y., Tsuboi, K., and Okubo, S.: Seasonal variation of enhancement ratios of trace gases observed over 10 years in the western North Pacific, *Atmos. Environ.*, 45, 2129–2137, doi:10.1016/j.atmosenv.2011.01.043, 2011.](#)
- [Wofsy, S. C.: HIAPER Pole-to-Pole Observations \(HIPPO\): fine-grained, global-scale measurements of climatically important atmospheric gases and aerosols, *Phil. Trans. Roy. Soc. A: Math. Phys. Eng. Sci.*, 369, 2073–2086, 2011.](#)
- 20 Yoshida, Y., Ota, Y., Eguchi, N., Kikuchi, N., Nobuta, K., Tran, H., Morino, I., and Yokota, T.: Retrieval algorithm for CO₂ and CH₄ column abundances from short-wavelength infrared spectral observations by the Greenhouse gases observing satellite, *Atmos. Meas. Tech.*, 4, 717-734, 2011.
- Yoshida, Y. et al.: Improvement of the retrieval algorithm for GOSAT SWIR XCO₂ and XCH₄ and their validation using TCCON data, *Atmos. Meas. Tech.*, 6, 1533-1547, 2013.

Table 1. Pressure levels of retrieval grid layers of GOSAT/TANSO-FTS TIR V1 L2 CO₂ data focused on in this study.

<u>Layer level</u>	<u>Pressure level of each layer (hPa)</u>	<u>Lower pressure level (hPa)</u>	<u>Upper pressure level (hPa)</u>
<u>1</u>	<u>927.79</u>	<u>1165.91</u>	<u>857.70</u>
<u>2</u>	<u>795.08</u>	<u>857.70</u>	<u>735.64</u>
<u>3</u>	<u>682.10</u>	<u>735.64</u>	<u>630.96</u>
<u>4</u>	<u>585.63</u>	<u>630.96</u>	<u>541.17</u>
<u>5</u>	<u>502.47</u>	<u>541.17</u>	<u>464.16</u>
<u>6</u>	<u>430.97</u>	<u>464.16</u>	<u>398.11</u>
<u>7</u>	<u>369.64</u>	<u>398.11</u>	<u>341.45</u>
<u>8</u>	<u>314.23</u>	<u>341.45</u>	<u>287.30</u>
<u>9</u>	<u>262.10</u>	<u>287.30</u>	<u>237.14</u>
<u>10</u>	<u>216.36</u>	<u>237.14</u>	<u>195.73</u>

Table 2. Biases of GOSAT/TANSO-FTS TIR CO₂ data against CME AK CO₂ data in each season of 2010–2012 at 541–464 hPa (left side of each box) and at 464–398 hPa (right side of each box) where the largest biases occurred in most cases. 541–464 and 464–398 hPa correspond to retrieval layers 5 and 6, respectively. Biases could not be evaluated due to no coincident data in the JJA seasons of 2011 and 2012.

5

<u>DJF</u>	<u>MAM</u>	<u>40°S–20°S</u>		<u>20°S–20°N</u>		<u>20°N–40°N</u>		<u>40°N–60°N</u>	
<u>JJA</u>	<u>SON</u>								
<u>2010</u>		<u>-2.1/-2.5</u>	<u>-1.1/-1.6</u>	<u>-4.1/-3.9</u>	<u>-4.5/-3.8</u>	<u>-4.2/-3.9</u>	<u>-5.1/-5.1</u>	<u>-4.1/-4.1</u>	<u>-6.0/-5.8</u>
		<u>-2.1/-2.4</u>	<u>-4.9/-4.7</u>	<u>-7.0/-7.3</u>	<u>-4.2/-4.3</u>	<u>-4.3/-4.6</u>	<u>-3.2/-3.4</u>	<u>-5.0/-5.0</u>	<u>-3.6/-4.1</u>
<u>2011</u>		<u>-1.7/-2.9</u>	<u>-4.2/-4.1</u>	<u>-4.6/-4.2</u>	<u>-4.7/-4.6</u>	<u>-3.9/-3.7</u>	<u>-5.3/-5.4</u>	<u>-4.5/-4.8</u>	<u>-5.2/-5.1</u>
		<u>-3.3/-3.4</u>	<u>-5.7/-5.4</u>	=	<u>-5.6/-5.5</u>	<u>-5.1/-5.7</u>	<u>-3.2/-3.3</u>	<u>-4.4/-4.6</u>	<u>-3.3/-3.9</u>
<u>2012</u>		<u>-2.2/-3.1</u>	<u>-2.9/-3.4</u>	<u>-3.9/-3.9</u>	<u>-5.6/-5.7</u>	<u>-3.9/-3.8</u>	<u>-5.8/-5.9</u>	<u>-4.3/-4.6</u>	<u>-5.3/-5.5</u>
		<u>-4.9/-4.9</u>	<u>-5.3/-5.5</u>	=	<u>-5.9/-5.7</u>	<u>-5.8/-6.3</u>	<u>-5.2/-4.9</u>	<u>-6.4/-6.5</u>	<u>-6.4/-6.7</u>

Table 3. Mode values of frequency distributions of differences in monthly averaged CO₂ concentrations between original (top left boxes) or bias-corrected (top right boxes) GOSAT/TANSO-FTS TIR and NICAM-TM CO₂ data in each season of 2010–2012, shown in Figure 7. The mode values presented here indicate the center value of a bin with a width of 0.5 ppm; a bin of “0.0” ranges from -0.25 to +0.25 ppm. Ratios of numbers of data categorized into each of the mode values to numbers of all 2.5° gridded data for comparisons (bottom boxes) are shown in middle left (original) and right (bias-corrected) boxes.

<u>[original] mode value (ppm)</u>	<u>[bias-corrected] mode value (ppm)</u>								
<u>[original] frequency (%)</u>	<u>[bias-corrected] frequency (%)</u>	<u>DJF</u>		<u>MAM</u>		<u>JJA</u>		<u>SON</u>	
<u>number of all 2.5° gridded data</u>									
<u>2010</u>	<u>-2.0</u>	<u>0.5</u>	<u>-2.5</u>	<u>0.0</u>	<u>-2.5</u>	<u>0.0</u>	<u>-2.5</u>	<u>0.5</u>	
	<u>13.6</u>	<u>13.9</u>	<u>10.5</u>	<u>12.9</u>	<u>10.7</u>	<u>10.4</u>	<u>11.8</u>	<u>11.1</u>	
	<u>641,427</u>		<u>947,983</u>		<u>1,176,998</u>		<u>1,279,370</u>		
<u>2011</u>	<u>-3.0</u>	<u>0.5</u>	<u>-3.5</u>	<u>1.0</u>	<u>-2.5</u>	<u>1.0</u>	<u>-2.5</u>	<u>0.5</u>	
	<u>11.3</u>	<u>12.1</u>	<u>8.8</u>	<u>11.4</u>	<u>9.8</u>	<u>9.4</u>	<u>11.5</u>	<u>9.4</u>	
	<u>1,156,444</u>		<u>1,093,808</u>		<u>1,156,010</u>		<u>1,222,288</u>		
<u>2012</u>	<u>-3.0</u>	<u>0.0</u>	<u>-4.0</u>	<u>0.0</u>	<u>-3.5</u>	<u>1.0</u>	<u>-4.0</u>	<u>0.5</u>	
	<u>12.1</u>	<u>13.1</u>	<u>8.7</u>	<u>11.8</u>	<u>9.3</u>	<u>10.5</u>	<u>10.6</u>	<u>10.5</u>	
	<u>1,050,530</u>		<u>1,010,457</u>		<u>1,148,979</u>		<u>1,117,909</u>		

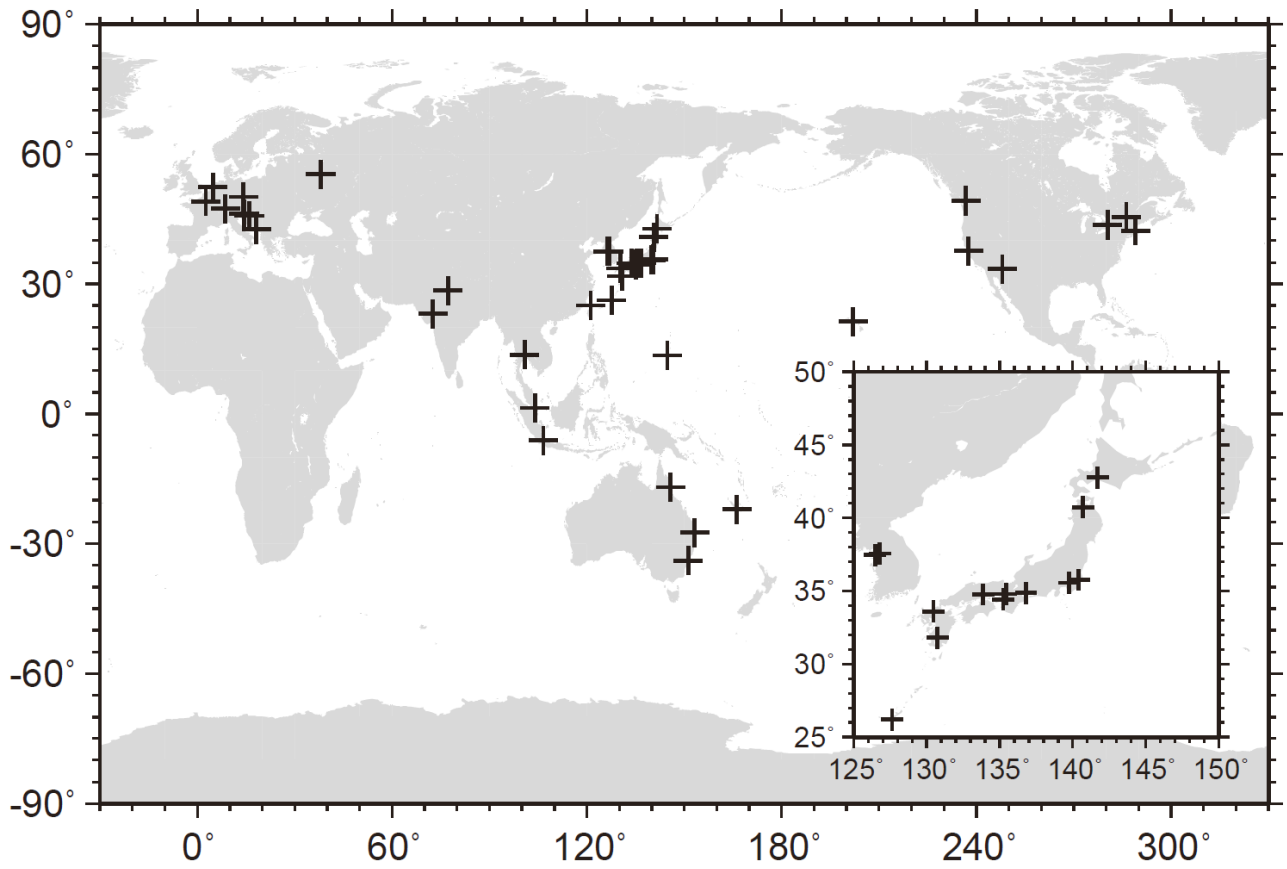


Figure 1. Locations of airports at which CONTRAIL CME ascending and descending observations were collected used infor
 5 this study.

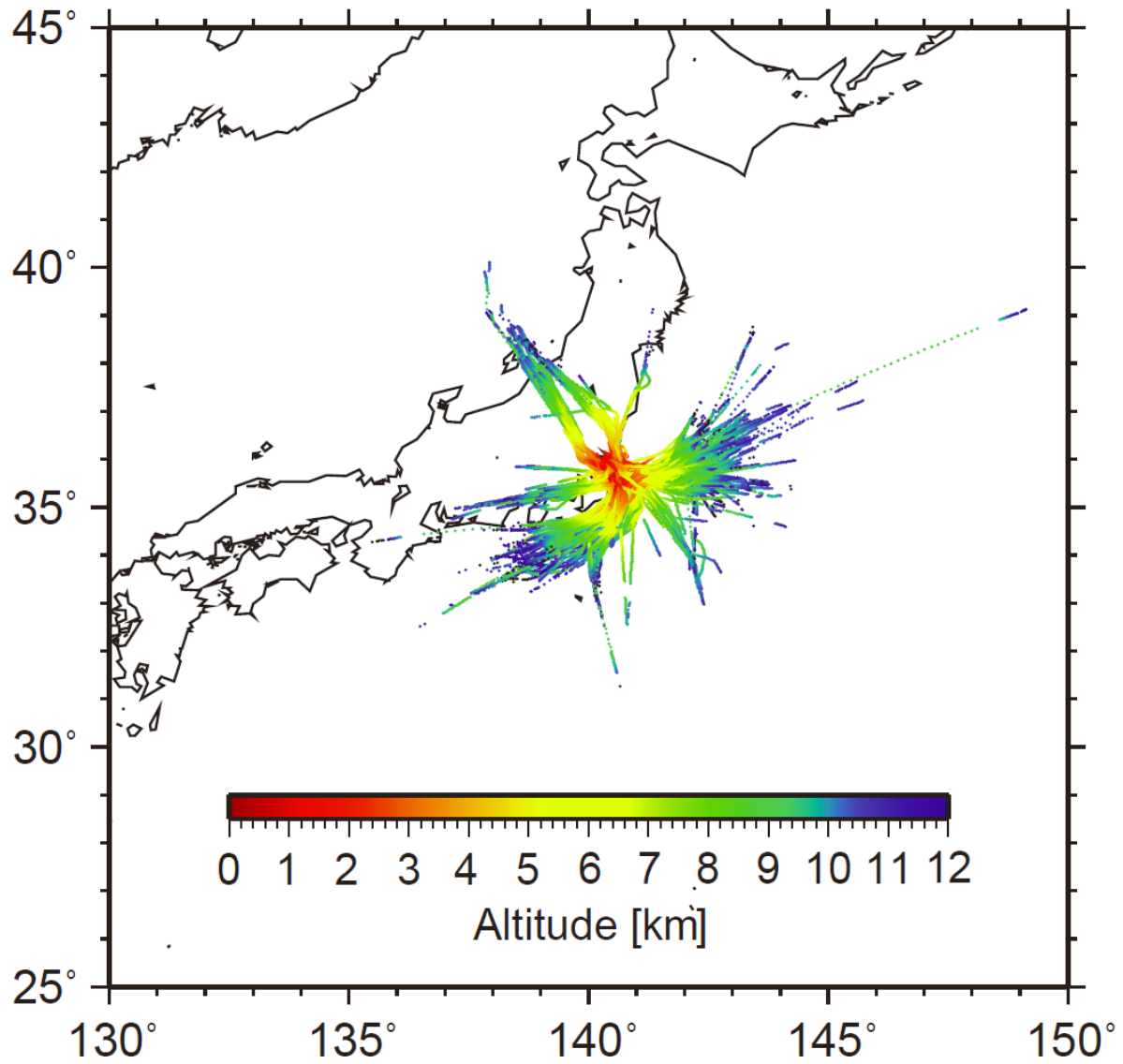
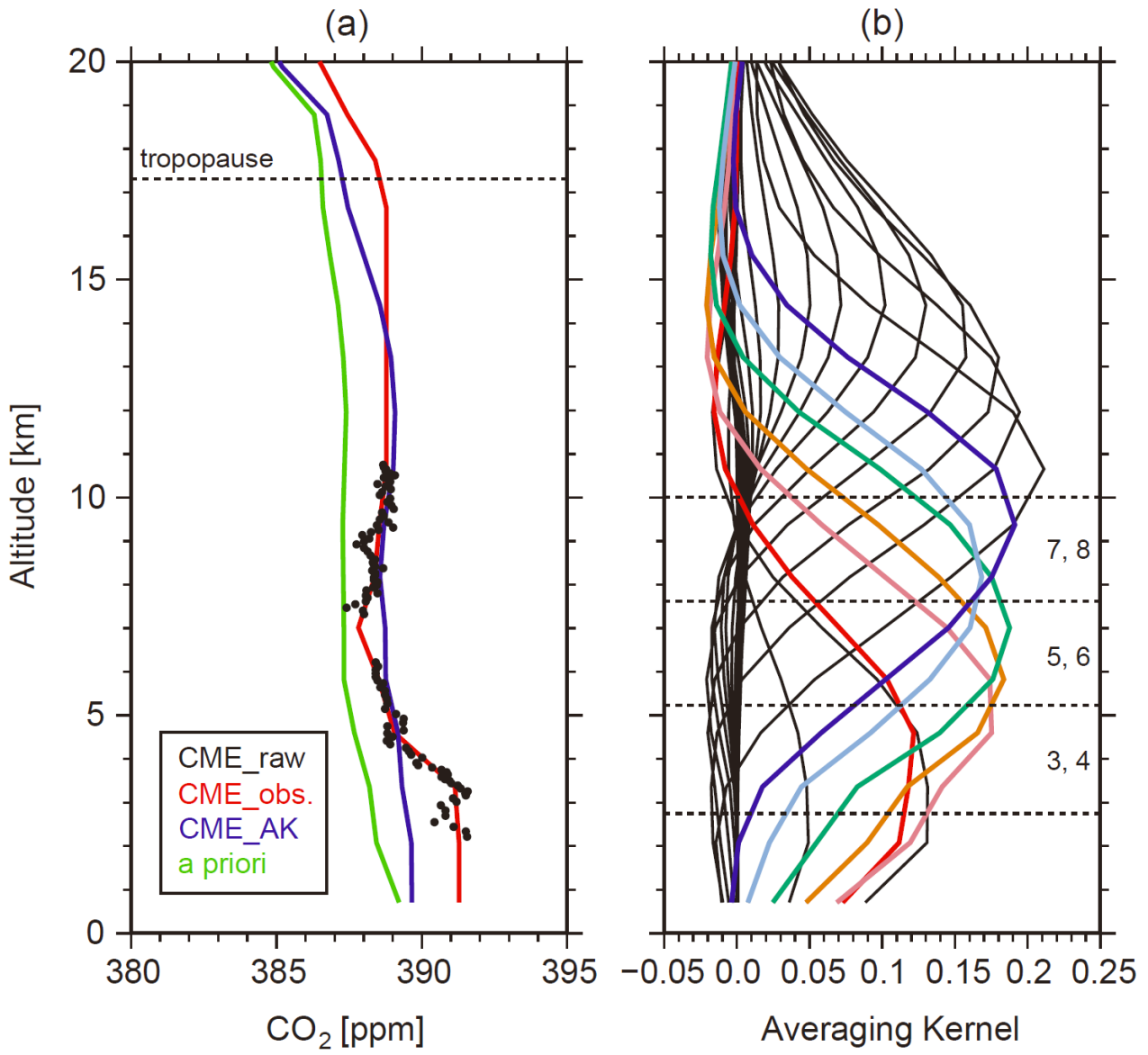
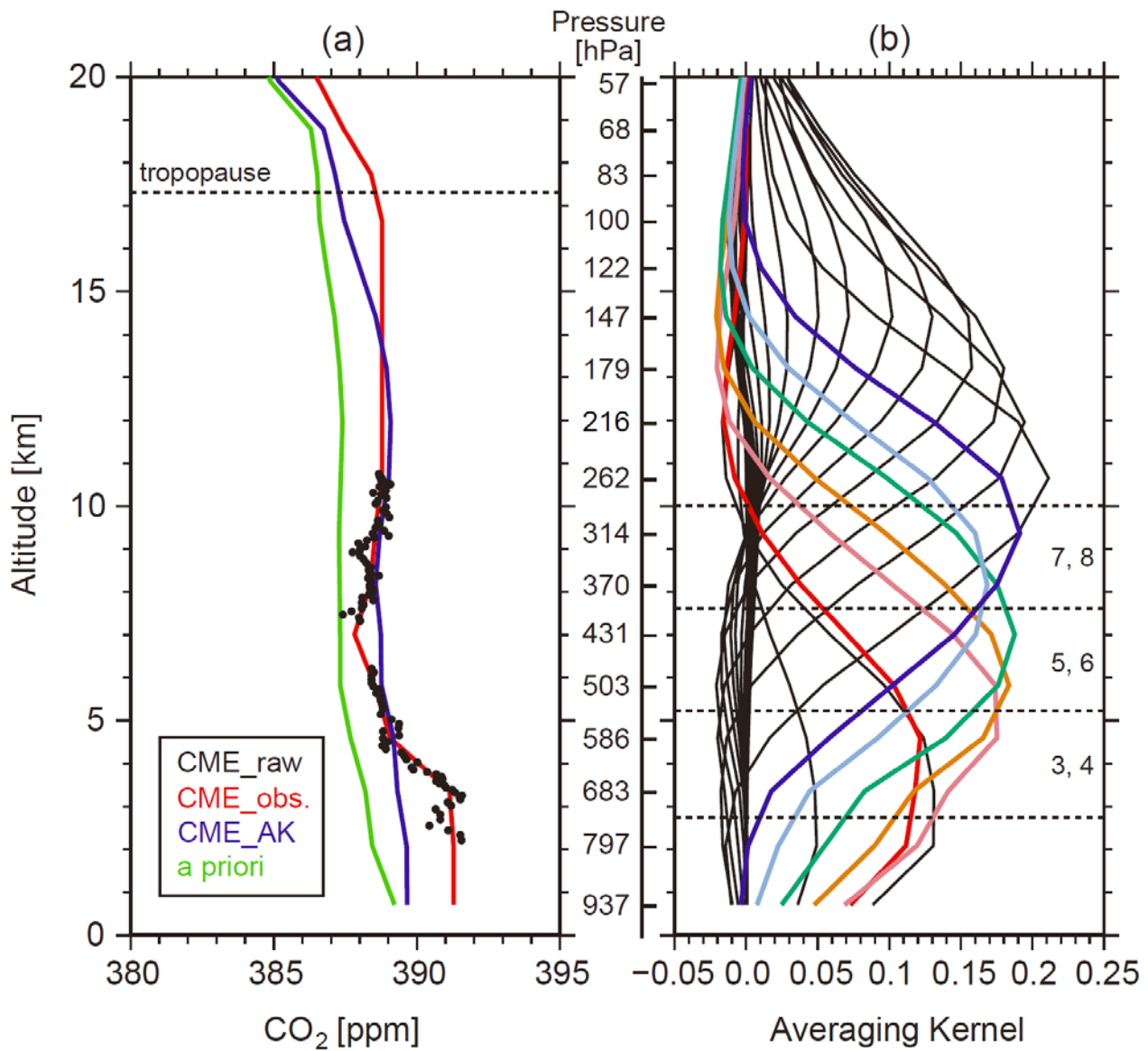
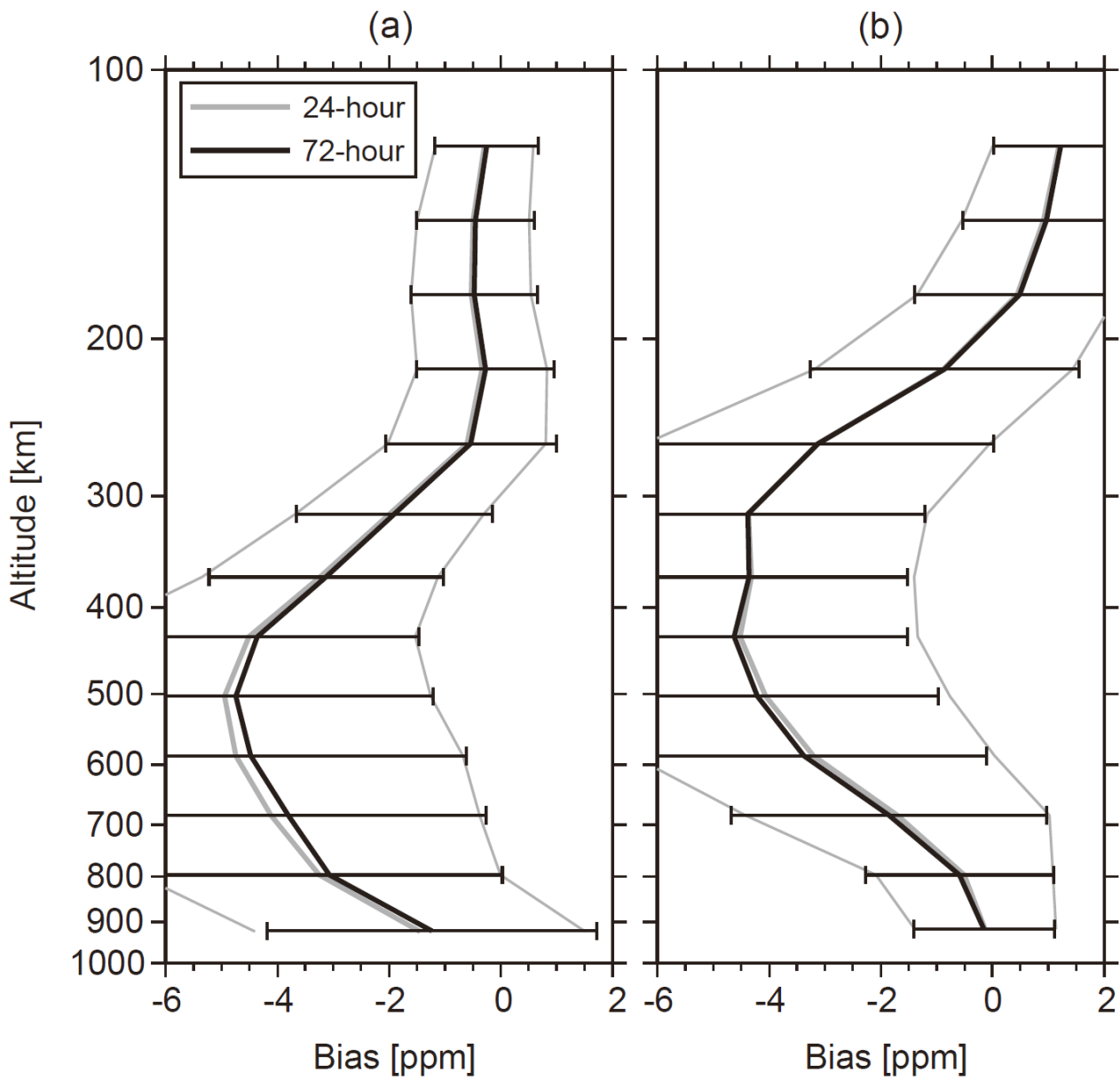


Figure 2. Flight tracks of all CME ascending and descending observations over Narita airport in 2010. Color indicates the
5 altitude levels of each flight.





5 Figure 3. (a) Black circles represent original CME data (CME_raw), the red line shows an interpolated profile of the CME data into GOSAT/TANSO-FTS TIR CO₂ 28 retrieval grid layers (CME_obs.), and the blue line shows the interpolated profile to which TIR averaging kernel functions, shown in panel (b), are applied (CME_AK), and the green line shows a priori CO₂ profile.



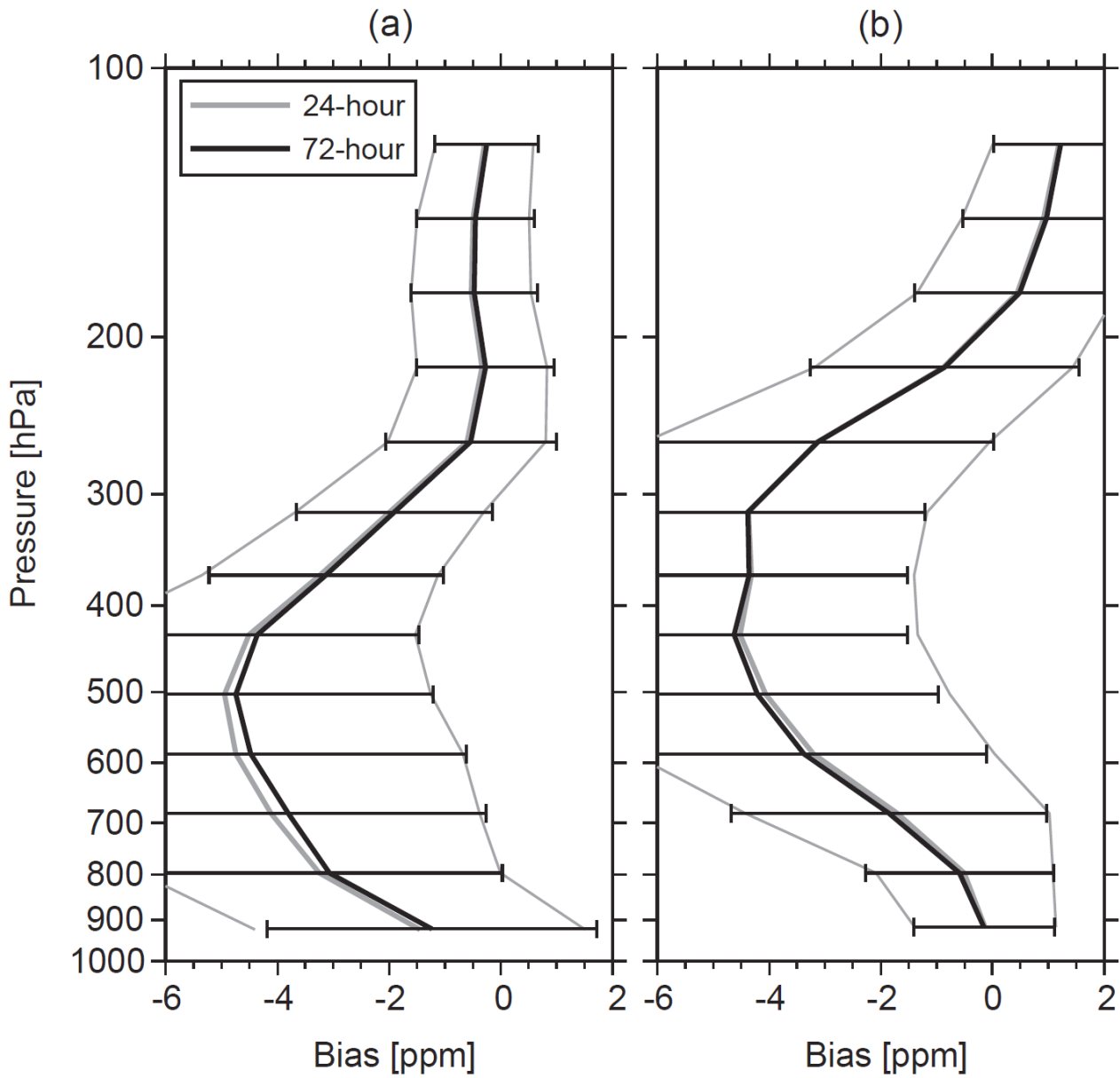


Figure 4. Bias profiles of GOSAT/TASNO-FTS TIR CO₂ data against CME_AK CO₂ data over Narita airport ([Japan](#)) using coincident pairs with 24-hour (gray) and 72-hour (black) time difference criteria: (a) winter (JF) 2010 and (b) summer (JJA)

5 2010.

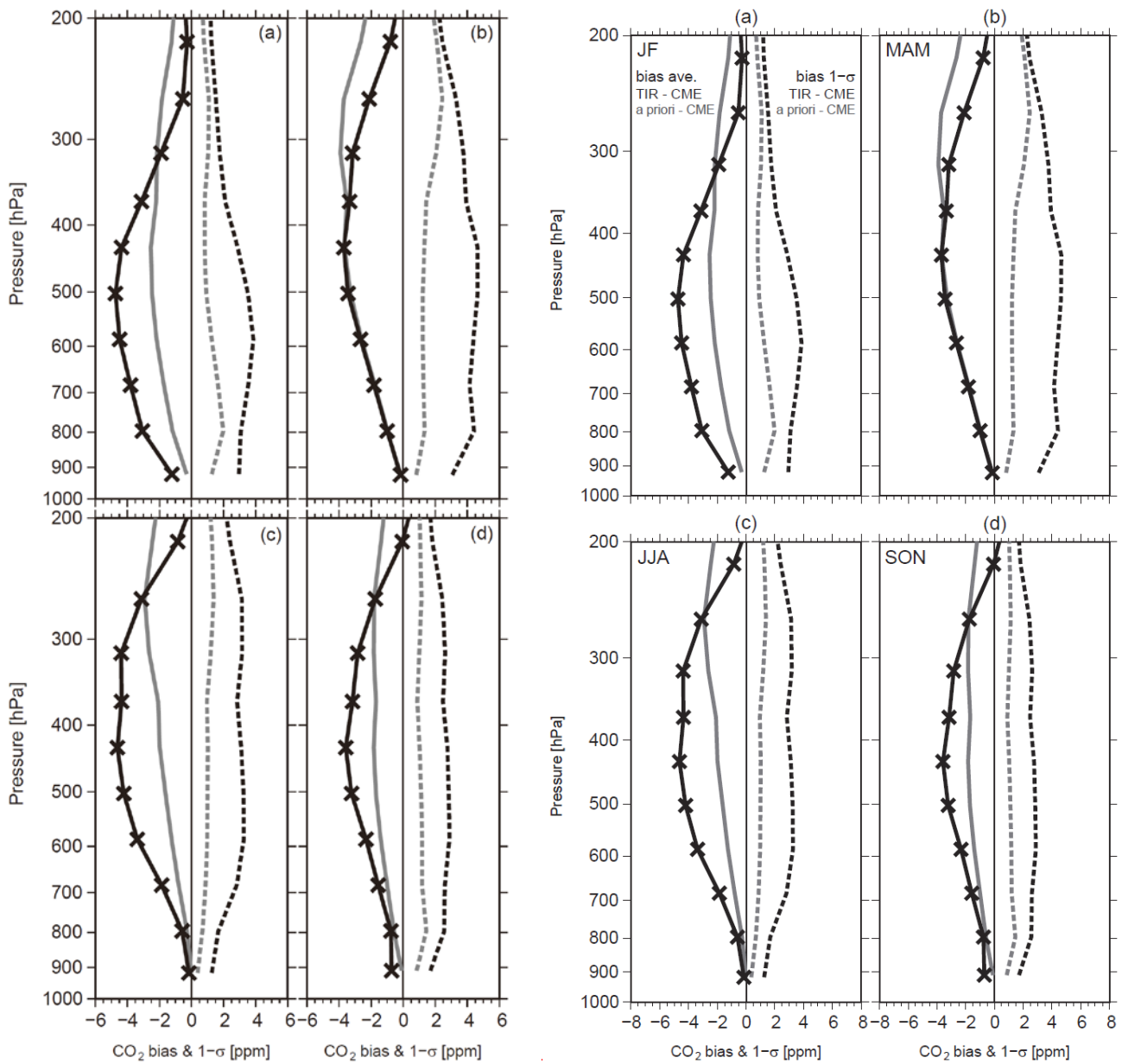
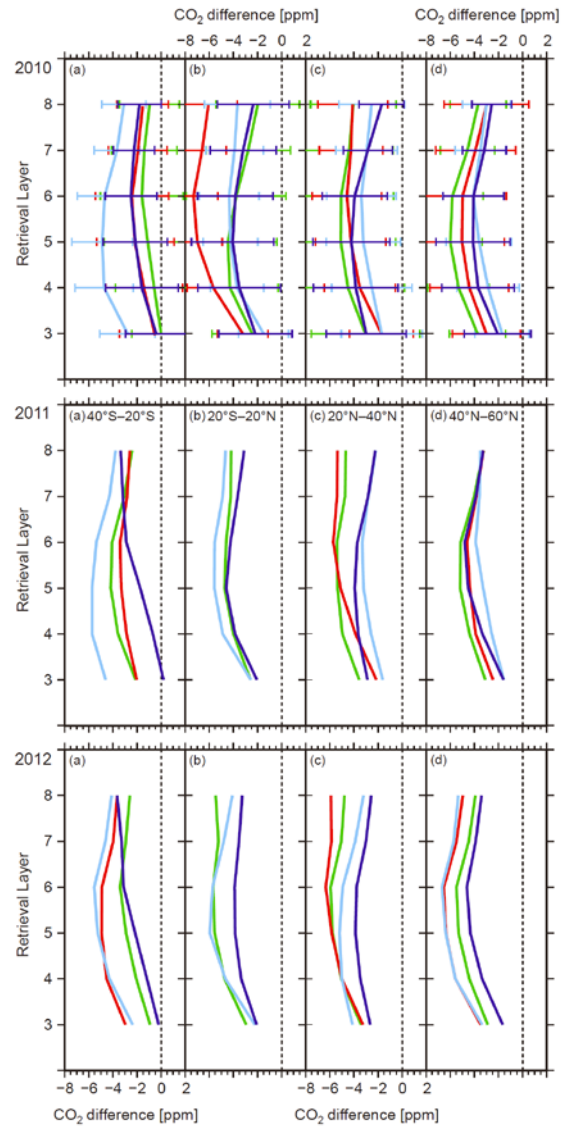
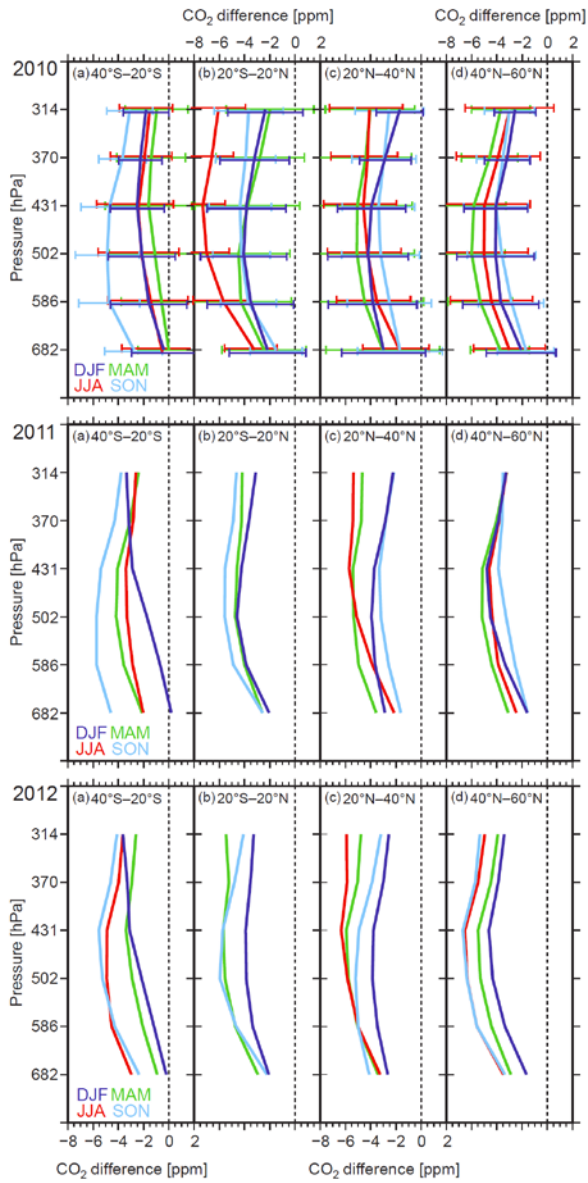


Figure 5. Bias profiles of GOSAT/TANSO-FTS TIR CO₂ data and a priori CO₂ data against CME_AK CO₂ data over Narita airport and the 1- σ standard deviations for each retrieval layer and season in 2010. The CME_AK CO₂ data are CME CO₂ data to which TIR CO₂ averaging kernel functions are applied. Solid black and gray lines indicate the biases of TIR and a priori CO₂ data, respectively, and dotted black and gray lines show their 1- σ standard deviations. Cross symbols indicate the center pressure level of each retrieval layer: (a) JF, (b) MAM, (c) JJA, and (d) SON.



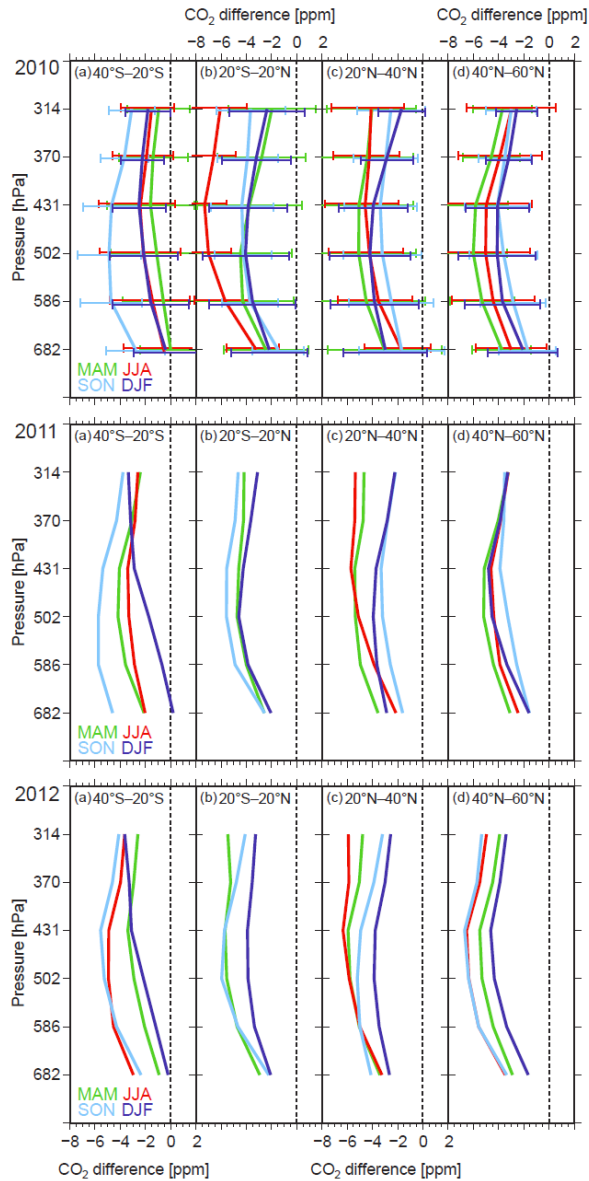
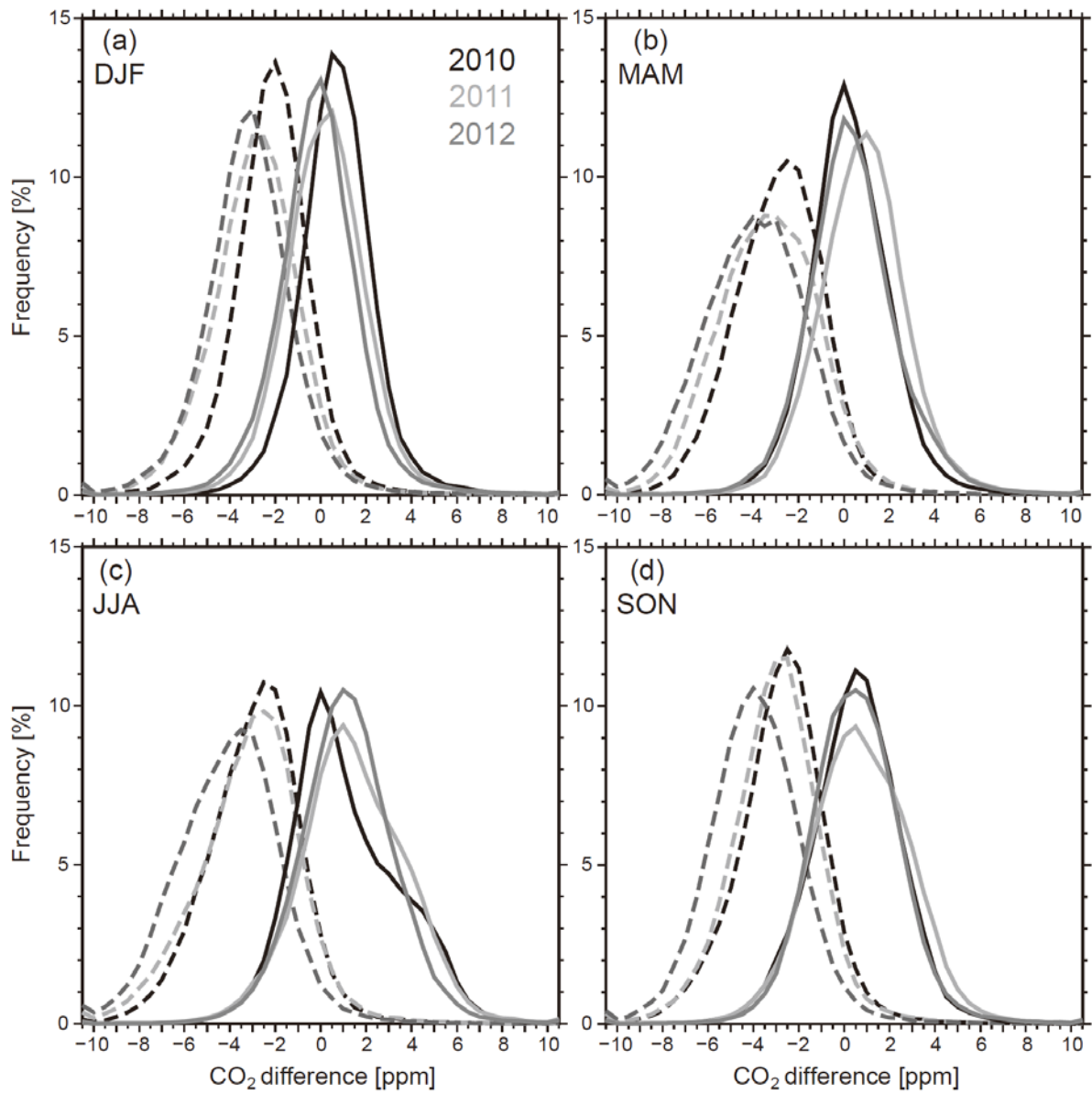
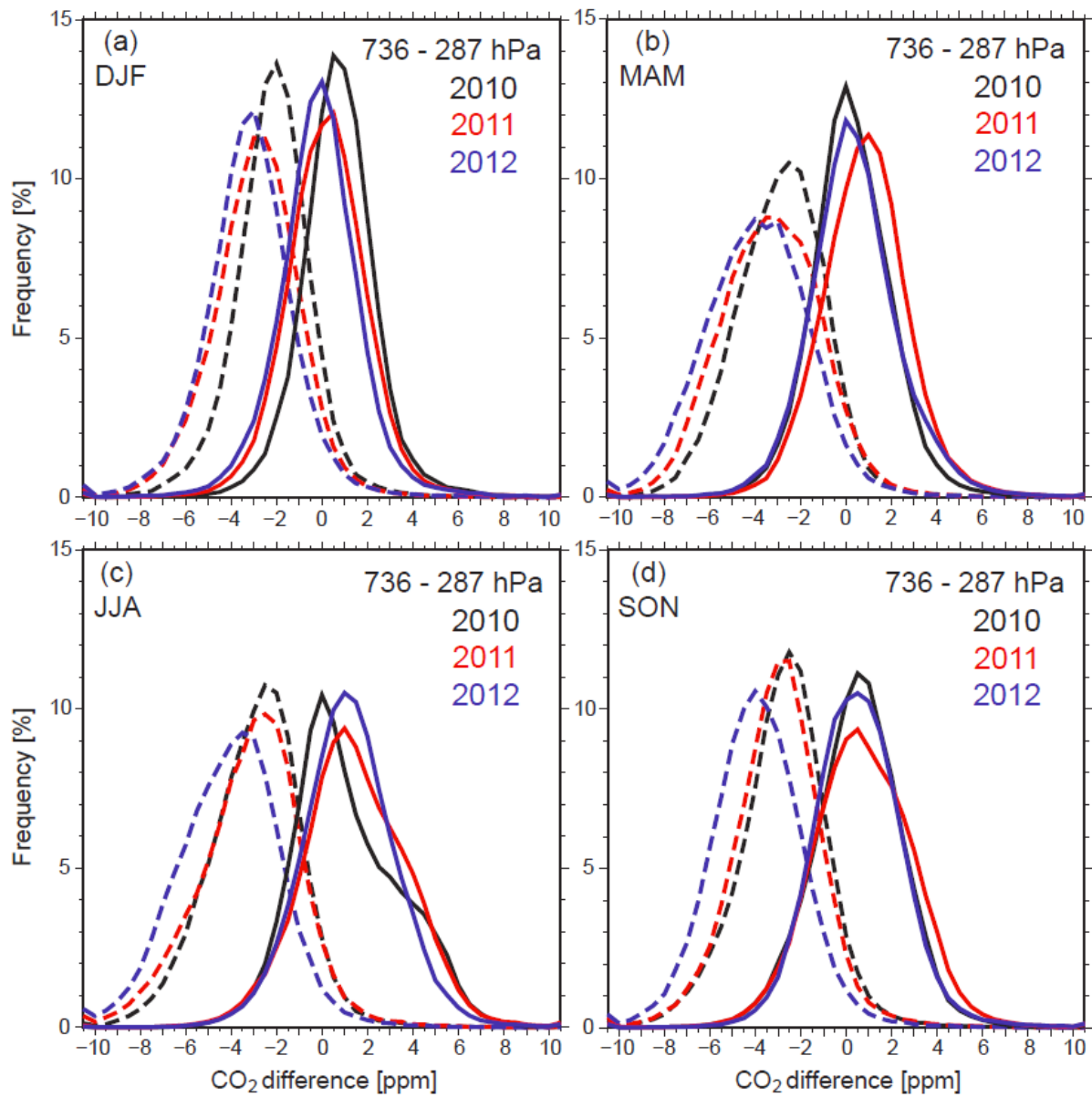


Figure 6. Average differences in CO₂ concentrations between GOSAT/TANSO-FTS TIR and CME_AK CO₂ data (TIR minus CME_AK) from 736 to 287 hPa (in-retrieval layers 3 to 8 (736–287 hPa)) for each latitude band and season, 2010–2012. The 1- σ standard deviations of the averages are indicated by horizontal bars for comparison of 2010 as a reference, which are slightly shifted up and down for visibility. We divided the data into four latitude bands: (a) 40°S–20°S, (b) 20°S–20°N, (c) 20°N–40°N, and (d) 40°N–60°N. Green, red, light blue, and blue lines represent the results in northern spring (MAM), northern summer (JJA), northern fall (SON), and northern winter (DJF), respectively.





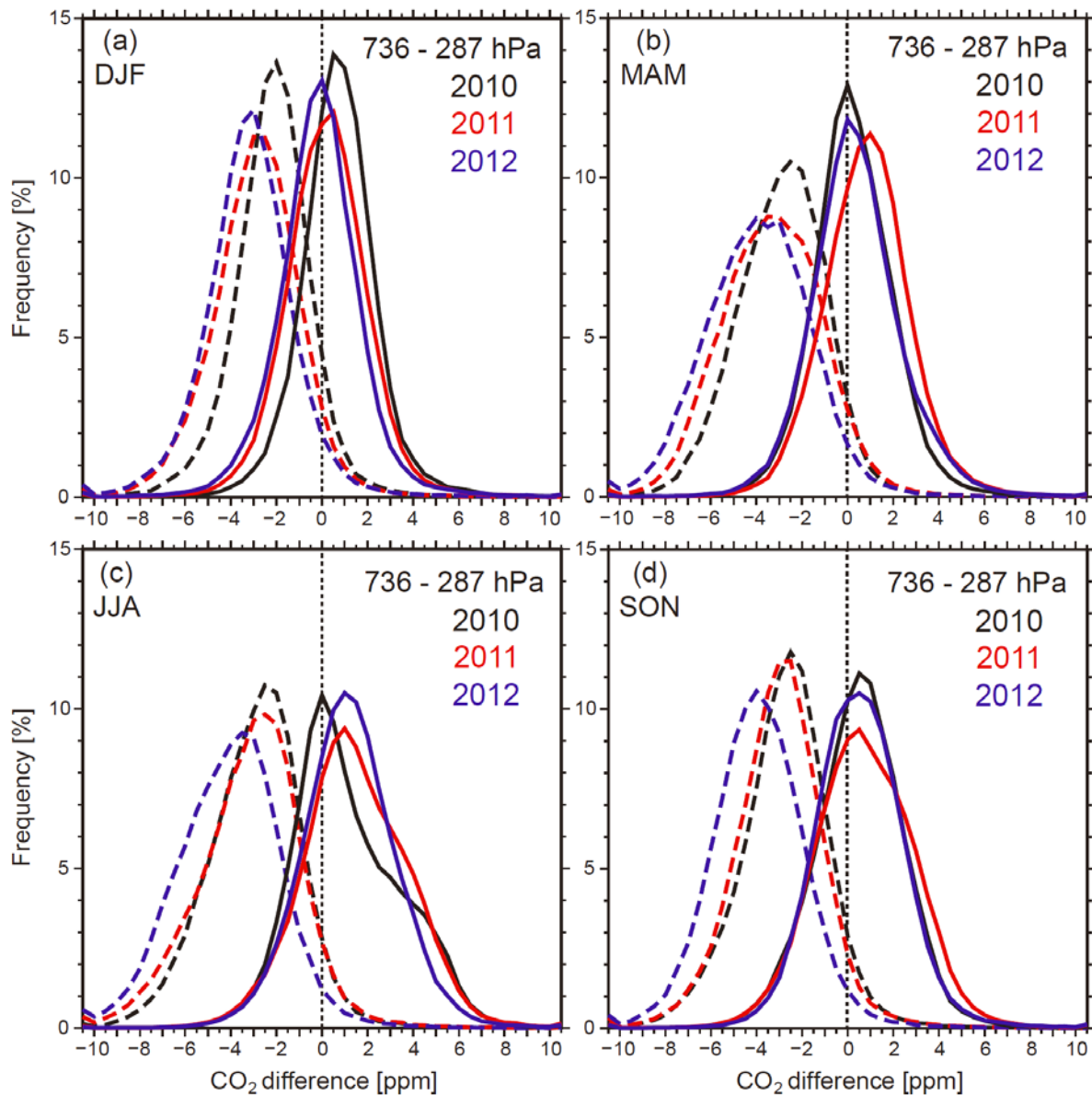
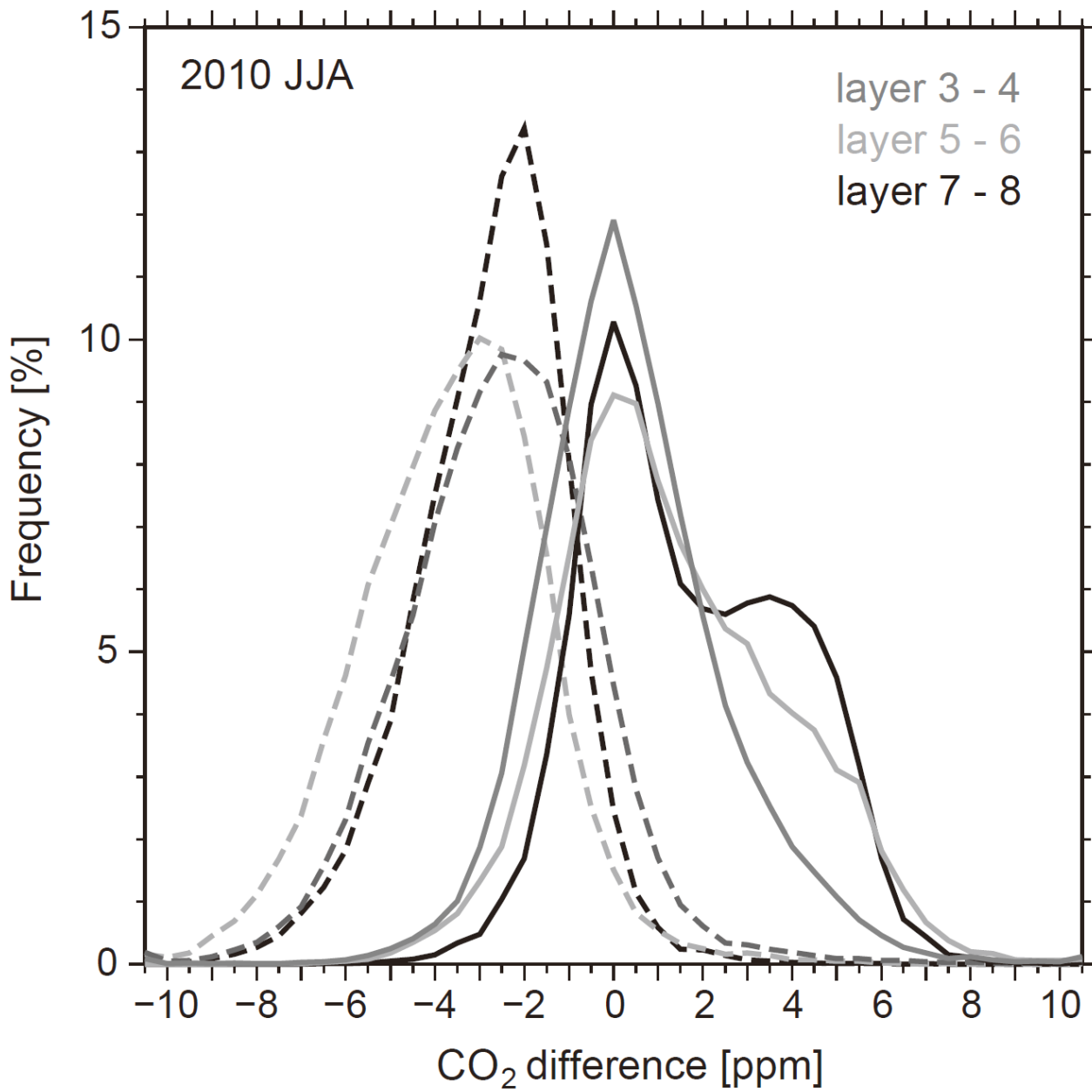
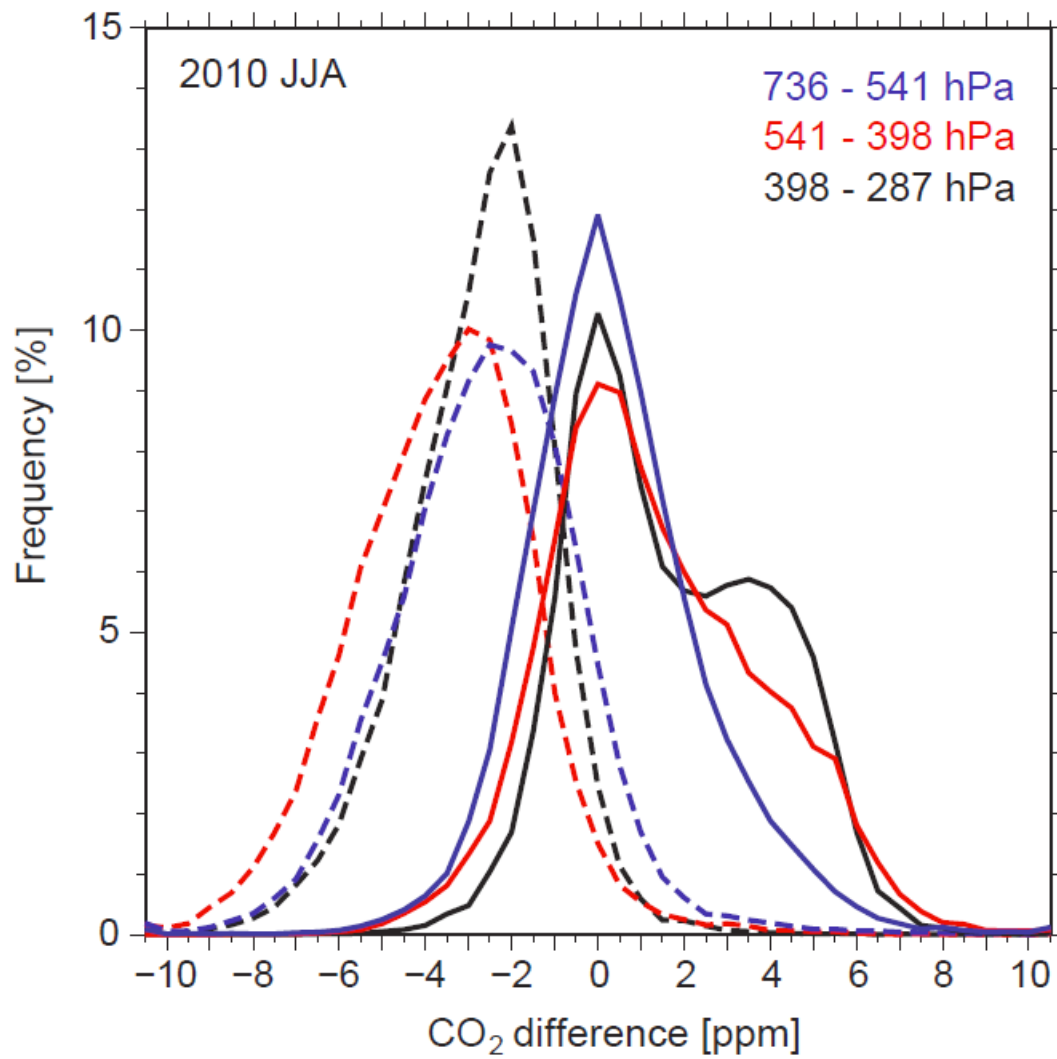


Figure 7. Frequency distributions of biases of monthly averaged GOSAT/TANSO-FTS TIR CO₂ data against monthly averaged NICAM-TM CO₂ data evaluated for each of retrieval layers from 736 to 287 hPa for each 2.5° grid in the latitude range of 40°S–60°N. Monthly averaged TIR CO₂ averaging kernel functions were applied to NICAM-TM CO₂ data in each grid. ~~Thick and dashed~~ Dashed and solid lines indicate the biases of the original TIR CO₂ data (no bias correction) and bias-corrected TIR CO₂ data, respectively. Black, ~~red~~ light gray, and ~~blue~~ dark gray lines show results from 2010, 2011, and 2012, respectively.





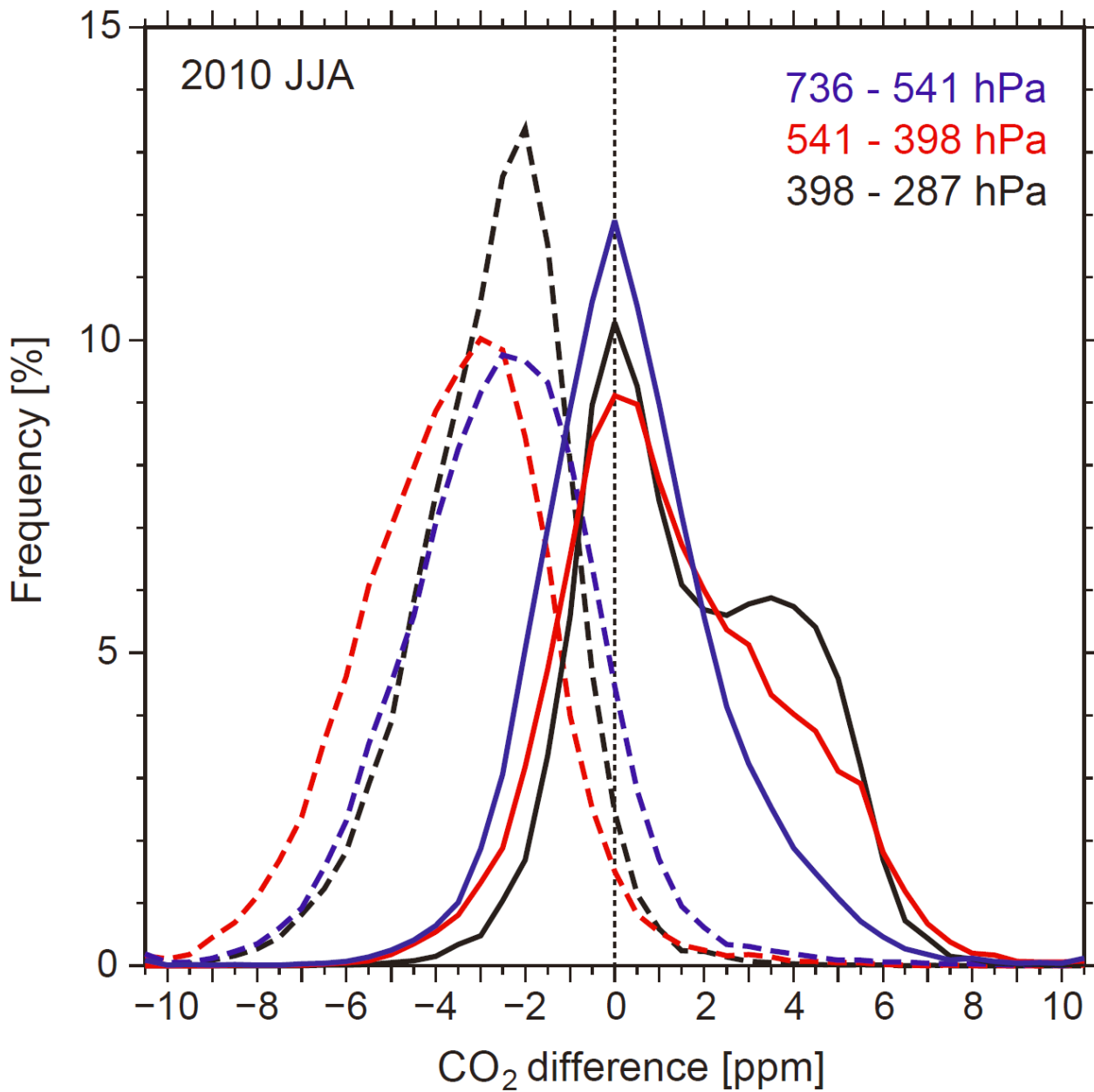
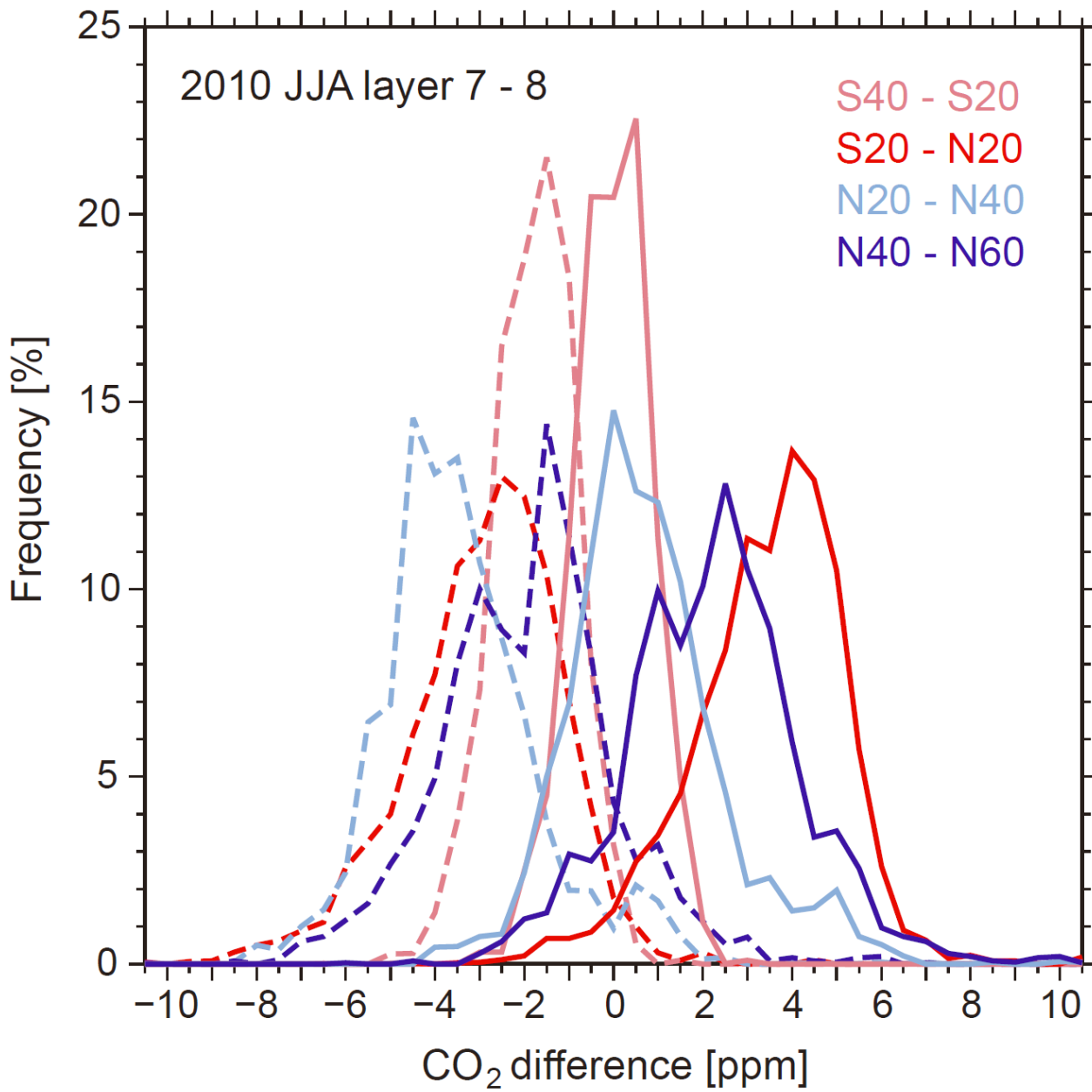
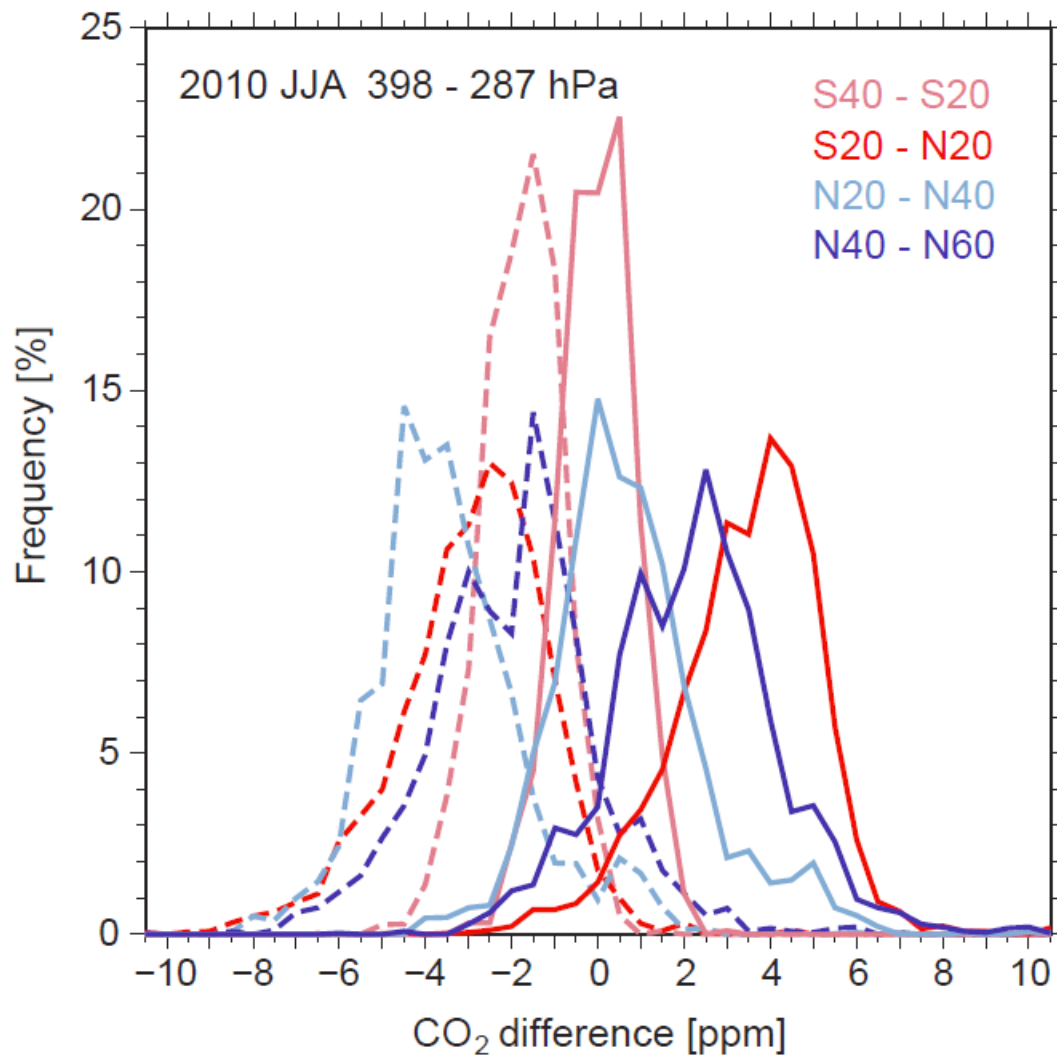


Figure 8. Same as Figure 7, but showing frequency distributions during the JJA season of 2010 on 736–541 hPa (~~for~~ retrieval layers ~~of~~ 3–4 (~~736–541 hPa~~), 5–6 (~~541–398 hPa~~ (retrieval layers), 5–6), and 7–8 (~~398–287 hPa~~ (retrieval layers), 7–8)). Black, ~~red~~ light gray, and ~~blue~~ dark gray lines indicate the results on in layers ~~3987–287 hPa~~ 8, ~~5415–398 hPa~~ 6, and ~~7363–541 hPa~~ 4, respectively.





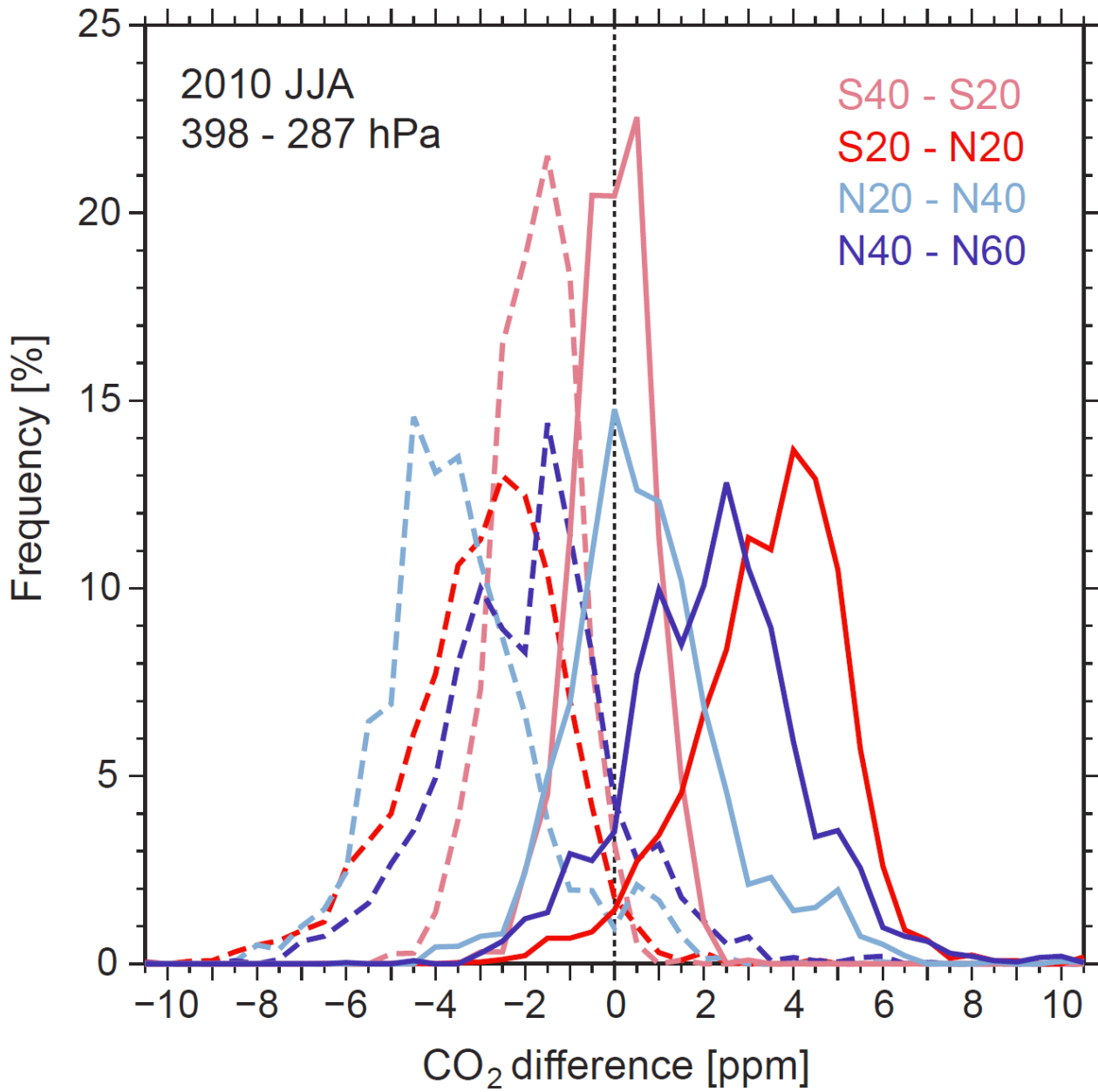
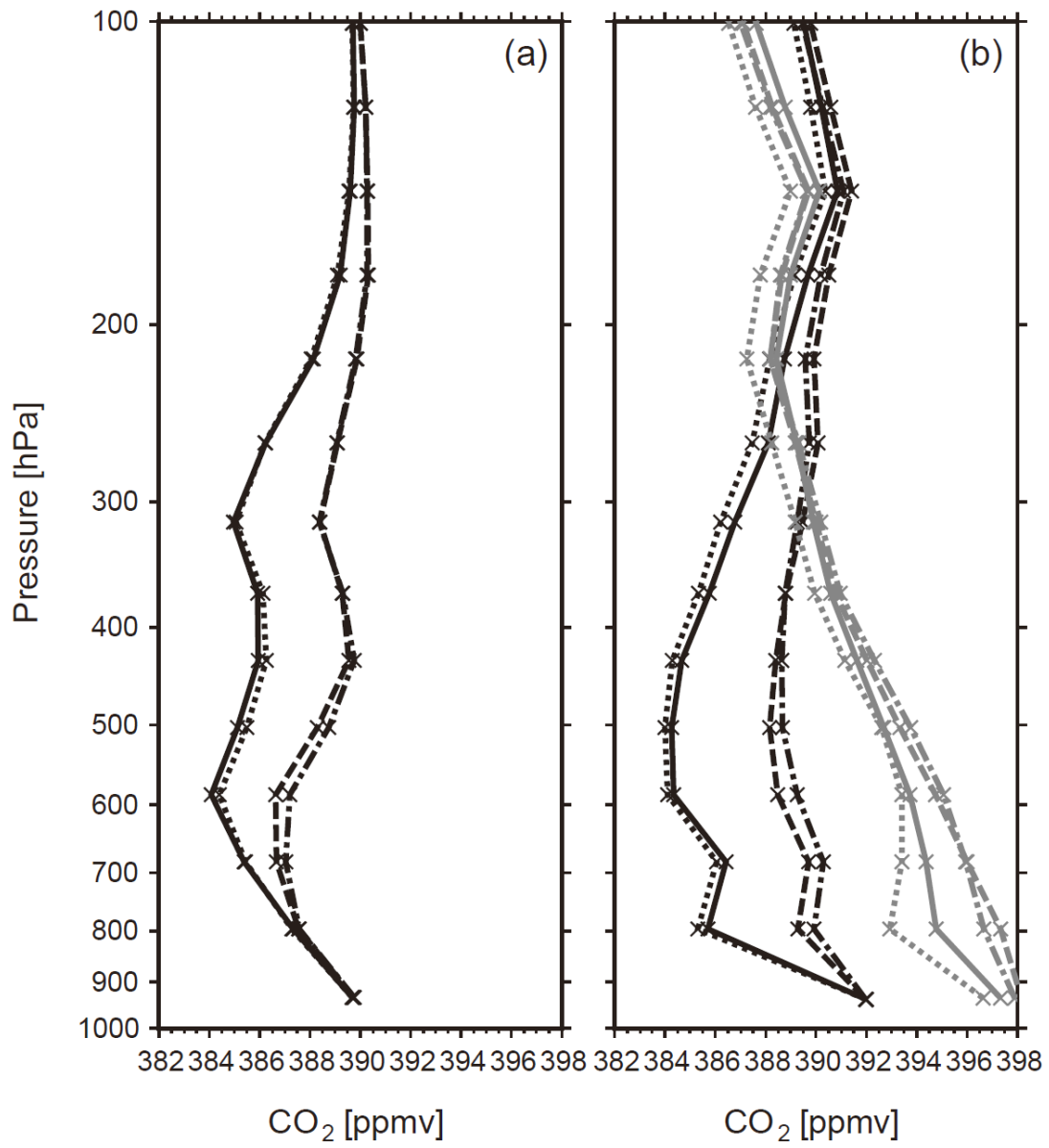


Figure 9. Same as Figure 7, but showing frequency distributions during the JJA season of 2010 on 398–287 hPa (for retrieval layers 7–8) for each latitude band. Pink, red, light blue, and blue lines shows the results from 40°S–20°S, 20°S–20°N, 20°N–40°N, and 40°N–60°N, respectively.



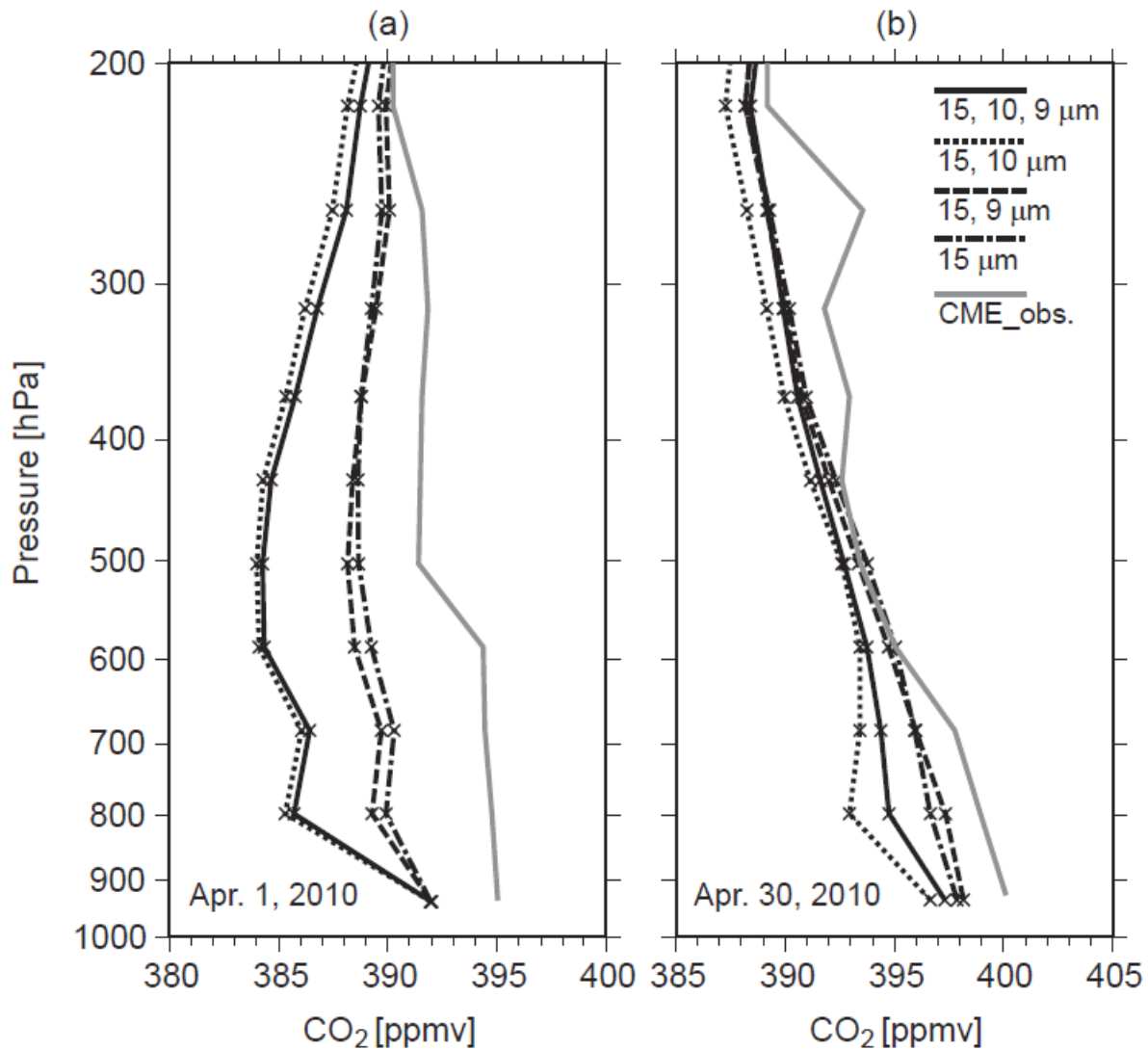


Figure 10. CO₂ profiles over Narita airport retrieved using four different wavelength bands of GOSAT/TANSO-FTS V161 L1B spectra: three bands, 15-μm, 10-μm, and 9-μm (solid thick lines); two bands, 15-μm and 10-μm (dotted lines); two bands, 15-μm and 9-μm (dashed lines), and the 15-μm band only (dashed-dotted lines). Nearby CME CO₂ profiles (CME_obs.) are shown by gray lines: (a) a case of April 1, 2010 ~~A case in low latitudes in summer (July) and~~ and (b) at two cases of April 30, 2010 ~~in northern middle latitudes in spring (April).~~

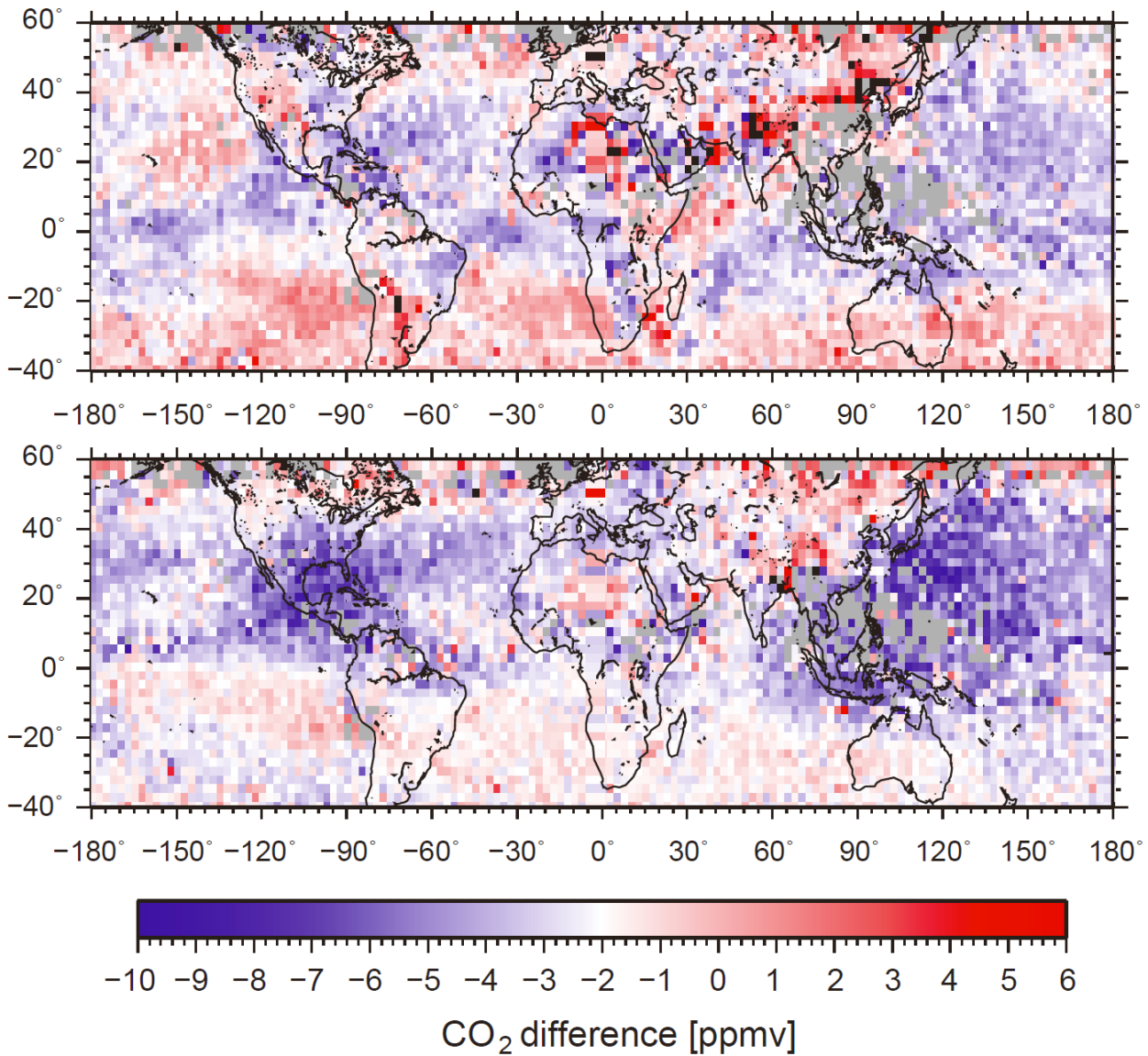


Figure 11. Latitude-longitude cross-sections of differences in monthly averages of GOSAT/TANSO-FTS TIR CO₂ data and
 5 NICAM-TM CO₂ data with considering TIR CO₂ averaging kernel functions (TIR minus NICAM-TM) in July 2010. The
 upper and lower panels show the results [on 682 hPa \(in-retrieval layer 3 \(736–631 hPa\)\)](#) and [314 hPa \(retrieval layer](#)
[8 \(834–287 hPa\)\)](#), respectively. [There are no GOSAT/TANSO-FTS TIR CO₂ data in gray-shaded areas.](#)